J. Fluid Mech. (2002), *vol.* 465, *pp.* 157–190.
DOI: 10.1017/S0022112002001064 Printed in the United Kingdom

Linear processes in stably and unstably stratified rotating turbulence

By H. HANAZAKI

Institute of Fluid Science, Tohoku University, 2-1-1 Katahira, Aoba-ku, Sendai, 980-8577, Japan

(Received 28 September 2000 and in revised form 1 March 2002)

Unsteady turbulence in stably and unstably stratified flow with system rotation around the vertical axis is analysed using the rapid distortion theory (RDT). Complete linear solutions for the spectra, variances and covariances are obtained analytically, and their characteristics, including the short- and long-time asymptotics and the effect of initial conditions, are examined in detail. It has been found that the rotation modifies the energy partition among the three kinetic energy components and the potential energy, and the ratio of the Coriolis parameter f to the Brunt–Väisälä frequency N, i.e. f/N, determines the final steady values of these components. The ratio also determines the phase of the energy/flux oscillation. Depending on whether $f/N > 1$ or $f/N < 1$, there is a phase shift of $\pm\pi/4$. However, unsteady aspects are largely dominated by stratification. This occurs because the effects of the Coriolis parameter f appear only in the form of fk_3, which vanishes for the horizontal wavenumber components ($k_3 = 0$), which contribute most to the energies and the fluxes. For example, the oscillation frequency of the energies and the fluxes asymptotes to $2N$ over a long time, in agreement with the stratified non-rotating turbulence. The initial time development is also dominanted by the stratification, and the short-time asymptotics ($Nt, ft \ll 1$) agree with those for non-rotating stratified fluids in the lowest-order approximation. In the special case of $f = N$, all the wavenumber components oscillate in phase, leading to no inviscid decay of oscillation. This is in contrast to the general case of $f \neq N$, in which inviscid decay has been observed. For pure rotation ($f \neq 0$, $N = 0$), analytical solutions showed that any turbulence that is initially axisymmetric around the rotation axis recovers exact three-dimensional isotropy in the kinetic energy components. Comparison with previous DNS and experiments shows that many of the unsteady aspects of the kinetic and potential energies and the vertical density flux can be explained by the linear processes described by RDT. Even the time development of the vertical vorticity, which would represent the small-scale characteristics of turbulence, agrees well with DNS. For unstably stratified turbulence, the initial processes observed in DNS and experiments, such as the initial decay of the kinetic energy due to viscosity and the subsequent rapid growth of the vertical kinetic energy compared to the horizontal kinetic energy, could be explained by RDT.

1. Introduction

There have been many studies on stably stratified turbulence. The first direct numerical simulation (DNS) was carried out by Riley, Metcalfe & Weissman (1981); it showed the importance of unsteadiness in stratified turbulence. They also proposed the notion of wave/vortex decomposition which is based on the Helmholtz

decomposition of an arbitrary vector, and which decomposes the velocity into vortex components with vertical vorticity and wave components with only horizontal vorticity. If time is scaled by the eddy overturning time and approximate hydrostatic balance is assumed, the governing equations reduce to the equations which describe the vortex components with only horizontal motion in the limit of small Froude number ($Fr \to 0$) (McWilliams 1995; Embid & Majda 1996, 1998; Riley & Lelong 2000). Since then, there have been many DNS studies, including those by Métais & Herring (1989), Gerz & Yamazaki (1993), Kimura & Herring (1996) and Staquet & Godeferd (1998). The notion of wave/vortex decomposition explained qualitatively the DNS results by Métais & Herring (1989) for finite $Fr(\neq 0)$, in which only the internal wave mode oscillated, while the vortex mode simply decayed due to viscosity and diffusion.

In laboratory experiments, Komori *et al.* (1983) found a counter-gradient density flux, a vertical turbulent flux in the opposite direction to the flux due to the molecular diffusion, which makes the turbulent diffusion coefficient negative. Itsweire, Helland & Van Atta (1986), Lienhard & Van Atta (1990), Yoon & Warhaft (1990) and Komori & Nagata (1996), among others, investigated in detail the time development of the kinetic and potential energies, vertical density flux and their spectra.

These results all showed the peoriodic oscillation of the vertical density flux. Hunt, Stretch & Britter (1988) used rapid distortion theory (RDT) which is a linear theory, and succeeded in predicting the oscillation of the energies and the fluxes. Hanazaki & Hunt (1996) solved the RDT equation analytically and showed that the periodic oscillation is the result of linear buoyant oscillation. They also showed, by applying the method of steepest descents/stationary phase, that the decaying oscillation observed in DNS and experiments occurs even in an inviscid fluid. This is because the wavenumber components with different directions have different periods of oscillation and only the horizontal wavenumber components ($k_3 = 0$) with vertical fluid motion at the slowest frequency N contribute to the energy/flux over a long time. Similar phenomenon in the context of diffusion were later called phase mixing by Kaneda & Ishida (2000).

The previous RDT results have shown the importance of initial conditions, such as the initial ratio of kinetic energy to potential energy, in determining the subsequent time development of stratified turbulence. They explained the difference in the direction and amplitude of the vertical density flux observed in the DNS (e.g. Gerz & Yamazaki 1993; Métais & Herring 1989) where the different initial energy ratio gave different subsequent time developments. Hanazaki & Hunt (1996) found, as an exception, that the long-time asymptotics of the ratio of the potential energy to the vertical kinetic energy ER ($\to 3/2$ as $t \to \infty$) is independent of the initial conditions. They also found that higher Prandtl number Pr generally gives stronger counter-gradient heat flux. This is also in agreement with the experiments which showed that for high Prandtl number flows, such as thermally stratified water flow ($Pr = 6$) or stratified salt water ($Pr = 600$), the counter-gradient flux was generally larger than in the wind tunnel experiments for heated air ($Pr = 0.7$). The RDT also succeeded in predicting the characteristics of the unsteady spectral behaviour which depend on the Prandtl number.

The suppression of vertical diffusion has been investigated by Kaneda & Ishida (2000) using the vertical velocities obtained by RDT to calculate the Eulerian and the Lagrangian two-time velocity correlations. They found good agreement with DNS under the condition of strong stratification. The characteristics of stratified turbulence with mean shear have also been investigated by Hanazaki & Hunt (2001).

Rotating turbulence has also been studied extensively. This includes the DNS by Bardina, Ferziger & Reynolds (1985), which showed the conservation of initial isotropy in rotating turbulence and the RDT studies by Cambon & Jacquin (1989), which investigated the effects of initial anisotropy on the time development of rotating turbulence. They found in their numerical solutions of the linearized equations that initially axisymmetric turbulence returns to isotropy in the energy components, while the anisotropy in the length scales increases with time. More recent studies include those by Cambon *et al.* (1994), Cambon, Mansour & Godeferd (1997) and Salhi & Cambon (1997).

On the other hand, studies of stratified rotating turbulence are relatively few. Bartello (1995) and Métais *et al.* (1996) utilized the wave/vortex decomposition in the analysis of DNS data for stratified rotating turbulence and investigated the nonlinear energy-transfer mechanisms. Bartello (1995) also investigated the time development of the kinetic and potential energy for $Pr = 1$ in decaying turbulence, which can be compared with the RDT results in this study. Recently Iida & Nagano (1999) and Tsujimura, Iida & Nagano (1998) investigated the same system using DNS for the case with rapid rotation, the results of which are compared in detail with the RDT results in this study. They also used some RDT solutions for the spectral components to explain the DNS results.

In this study we extend the results of Hanazaki (2000) where some inviscid results are obtained and solve the RDT equations as analytically as possible to theoretically clarify the essential mechanisms governing the transport processes in stratified rotating turbulence. We first obtain the most general analytical RDT solutions and use them to calculate the three-dimensional spectra, then integrate them to obtain the variances and covariances such as the vertical density flux and the kinetic/potential energies for initially isotropic and axisymmetric turbulence. We then investigated the asymptotic behaviour of those quantities and compared the results with DNS and experiments to clarify the heat/density transport mechanisms in stably stratified rotating turbulence.

To investigate the mechanisms which contribute to the fluxes, the energies, the three-dimensional and one-dimensional spectra observed in DNS and experiments, analytical integrations of the Fourier componemts are very useful. By examining the characteristics of the integral representations, we can identify which components contribute most to these quantities. This has been demonstrated in Hanazaki & Hunt (1996, 2001) for stratified turbulence with and without mean shear. While the linear theory often has limitations in its applicability, if the analytical expressions can be obtained, they are useful guides for both the DNS and the experiments. Thorough knowledge of the linear mechanisms could become the starting point for the studies of weak nonlinearity and then strong nonlinearity.

2. RDT equations

We consider a homogeneous turbulent flow with vertical density stratification ($\mathrm{d}\bar{\rho}/\mathrm{d}x_3$) and system rotation around the vertical axis. The governing equations in the rotating frame under the Boussinesq approximations are

$$\frac{\partial \boldsymbol{u}}{\partial t} + (\boldsymbol{u}\cdot\nabla)\boldsymbol{u} + 2\boldsymbol{\Omega}\times\boldsymbol{u} = -\frac{1}{\rho_0}\nabla p - g\hat{\boldsymbol{x}}_3\frac{\rho}{\rho_0} + \nu\nabla^2\boldsymbol{u}, \tag{2.1}$$

$$\frac{\partial \rho}{\partial t} + (\boldsymbol{u}\cdot\nabla)\rho + u_3\frac{\mathrm{d}\bar{\rho}}{\mathrm{d}x_3} = \kappa\nabla^2\rho, \tag{2.2}$$

and

$$\nabla\cdot\boldsymbol{u} = 0, \tag{2.3}$$

where ρ is the density perturbation from $\bar{\rho}(x_3)$, $\boldsymbol{u}$ is the velocity fluctuation, $\boldsymbol{\Omega}=(0,0,\Omega)$ denotes the angular velocity of the system rotation, g is the accerelation due to gravity, $\hat{\boldsymbol{x}}_3$ is the unit vector in the vertical upward direction, ρ_0 is the representative density, and ν and κ are the viscosity and diffusion coefficient respectively.

We linearize the above equations and introduce the following spectral decompositions (Batchelor & Proudman 1954; Townsend 1976):

$$u_i = \sum_{\boldsymbol{k}} \hat{u}_i(\boldsymbol{k},t)\mathrm{e}^{\mathrm{i}\boldsymbol{k}\cdot\boldsymbol{x}} \quad (i=1,2,3), \tag{2.4}$$

and

$$\frac{g}{\rho_0}\rho = \sum_{\boldsymbol{k}} \hat{\rho}(\boldsymbol{k},t)\,\mathrm{e}^{\mathrm{i}\boldsymbol{k}\cdot\boldsymbol{x}}. \tag{2.5}$$

We then obtain a set of ordinary differential equations (RDT equations) to be solved:

$$\left(\frac{\mathrm{d}}{\mathrm{d}t}+\nu k^2\right)\hat{u}_i + \left(\delta_{ij}-\frac{k_i k_j}{k^2}\right)\epsilon_{j3l} f \hat{u}_l = \left(\frac{k_i k_3}{k^2}-\delta_{i3}\right)\hat{\rho}, \tag{2.6}$$

and

$$\left(\frac{\mathrm{d}}{\mathrm{d}t}+\kappa k^2\right)\hat{\rho} = N^2\hat{u}_3, \tag{2.7}$$

where $f=2\Omega$ is the Coriolis parameter (twice the angular velocity Ω) and N is the Brunt–Väisälä frequency defined by $N^2=-(g/\rho_0)(\mathrm{d}\bar{\rho}/\mathrm{d}x_3)$.

We should note that in the above formulation the wavenumber does not change with time when there is no mean shear, i.e.

$$\frac{\mathrm{d}k_i}{\mathrm{d}t}=0, \tag{2.8}$$

so that

$$\boldsymbol{k}(t)=\boldsymbol{k}(0)=(k_1,k_2,k_3). \tag{2.9}$$

It is important to note the conditions for which the RDT in stably stratified rotating flow is valid. They are given by the conditions that the nonlinear term $(\boldsymbol{u}\cdot\nabla)\boldsymbol{u}$ ($\boldsymbol{u}=(u_1,u_2,u_3)$, $|\boldsymbol{u}|=O(u)$) in the Navier–Stokes equations is small compared to either the buoyancy term $g\rho/\rho_0$ (Derbyshire & Hunt 1993) or the Coriolis term $2\boldsymbol{\Omega}\times\boldsymbol{u}$. At the same time the term $(\boldsymbol{u}\cdot\nabla)\rho$ must be small compared to $u_3\mathrm{d}\bar{\rho}/\mathrm{d}x_3$ in the equation for the density.

Using the eddy size l and its characteristic velocity $u(l)$, the nonlinear term is expressed as

$$|(\boldsymbol{u}\cdot\nabla)\boldsymbol{u}| = O\left(\frac{u^2}{l}\right),$$

while the buoyancy term is (cf. Hanazaki & Hunt 1996)†

$$\begin{aligned}\frac{g}{\rho_0}\rho &= O(uN^2t)\ (\text{if } Nt, ft \ll 1\ (\text{cf. }\S 4.3)),\\ &= O(uN)\left(\text{if } Nt\geqslant 1 \text{ or } ft\geqslant 1\ (\text{cf. }\S 4.4.1,\ \text{eq. (4.21)}),\ \text{and } \frac{f}{N}<1\right),\\ &= O\left(uN\left(\frac{N}{f}\right)^{1/2}\right)\left(\text{if } Nt\geqslant 1 \text{ or } ft\geqslant 1,\ \text{and } \frac{f}{N}>1\right),\end{aligned}$$

† Here, the estimation of $(g/\rho_0)\rho$ was obtained using the RDT solutions given in §4. Therefore, the applicability conditions of RDT obtained here are the necessary conditions rather than the sufficient conditions.

and the Coriolis term is

$$2\boldsymbol{\Omega} \times \boldsymbol{u} = O(fu).$$

Then, at large times ($Nt \geqslant 1$ or $ft \geqslant 1$), if $f/N < 1$ is satisfied, $Fr_l(\equiv u/Nl) \ll 1$ or $Ro_l(\equiv u/fl) = Fr_l(N/f) \ll 1$, i.e. $Fr_l \ll 1$ is the necessary condition for the validity of (2.6). On the other hand, if $f/N > 1$, $Fr_l(f/N)^{1/2} = Ro_l(f/N)^{3/2} \ll 1$ or $Ro_l \ll 1$, i.e. $Ro_l \ll 1$ is the necessary condition for the validity of (2.6).

Using the estimation for the buoyancy term, the buoyancy advection term becomes

$$(\boldsymbol{u} \cdot \nabla)\rho = O\left(uNt\frac{\mathrm{d}\bar{\rho}}{\mathrm{d}x_3}\right) (\text{if } Nt, ft \ll 1 \text{ (cf. § 4.3)}),$$

$$= O\left(u\frac{u}{Nl}\frac{\mathrm{d}\bar{\rho}}{\mathrm{d}x_3}\right)\left(\text{if } Nt \geqslant 1 \text{ or } ft \geqslant 1 \text{ (cf. § 4.4.1), and } \frac{f}{N} < 1\right),$$

$$= O\left(u\frac{u}{Nl}\left(\frac{f}{N}\right)^{1/2}\frac{\mathrm{d}\bar{\rho}}{\mathrm{d}x_3}\right)\left(\text{if } Nt \geqslant 1 \text{ or } ft \geqslant 1, \text{ and } \frac{f}{N} > 1\right).$$

Then comparison with $u_3\mathrm{d}\bar{\rho}/\mathrm{d}x_3 = O(u\mathrm{d}\bar{\rho}/\mathrm{d}x_3)$ gives that at large times ($Nt \geqslant 1$ or $ft \geqslant 1$), if $f/N < 1$, $Fr_l \ll 1$ is the condition for the validity of (2.7) and if $f/N > 1$, $Ro_l(f/N)^{1/2} \ll 1$ is the condition for the validity of (2.7).

Therefore, the applicabitity conditions for which both (2.6) and (2.7) are valid are

$$Fr_l \ll 1 \text{ (if } f/N < 1),$$

$$Ro_l\left(\frac{f}{N}\right)^{1/2} = Fr_l\left(\frac{N}{f}\right)^{1/2} \ll 1 \text{ (if } f/N > 1).$$

Thus, if the stratification is dominant ($f/N < 1$), $Fr_l \ll 1$ is the applicability condition of RDT, but if the rotation is dominant ($f/N > 1$), Fr_l is not necessarily small but Ro_l must be very small for the validity of RDT. This suggests at the same time that in the limit of weak stratification ($N \to 0$), it becomes difficult to satisfy $Ro_l(f/N)^{1/2} \ll 1$, implying that the parameter region of applicability at small Ro_l might be narrower for pure rotating flows, although for those flows, the equation for the density does not exist and the applicability condition becomes just $Ro_l \ll 1$. If we denote the length scale and the velocity scale of energy-containing eddies by l_0 and $u_0(= u(l_0))$ respectively, the inverse of the time scale of each eddy with length scale l becomes

$$\frac{u}{l} = O\left(\frac{u_0}{l_0}\right) \text{(at low and moderate } Re),$$

$$= O(\epsilon^{1/3}l^{-2/3}) \text{ (at high } Re, \text{ where } \epsilon \text{ is the local turbulence energy dissipation rate).}$$

Then, if we define the turbulent Froude number $Fr(\equiv u_0/Nl_0)$ and the turbulent Rossby number $Ro(\equiv u_0/fl_0)$ based on the energy-containing eddies, we have at low and moderate $Re(\equiv u_0l_0/\nu)$,

$$Fr_l \sim Fr \quad \text{and} \quad Ro_l \sim Ro,$$

but at high Re,

$$Fr_l \sim \frac{\epsilon^{1/3}}{Nl^{2/3}} \sim Fr\left(\frac{l_0}{l}\right)^{2/3} \quad \text{and} \quad Ro_l \sim \frac{\epsilon^{1/3}}{fl^{2/3}} \sim Ro\left(\frac{l_0}{l}\right)^{2/3}.$$

The above applicability conditions can be rewritten using Fr and Ro and they become at low and moderate Re

$$Fr \ll 1 \left(\text{if } \frac{f}{N} < 1\right),$$

or

$$Ro \left(\frac{f}{N}\right)^{1/2} = Fr \left(\frac{N}{f}\right)^{1/2} \ll 1 \left(\text{if } \frac{f}{N} > 1\right),$$

while at high Re they become

$$Fr \left(\frac{l_0}{l}\right)^{2/3} \ll 1 \left(\text{if } \frac{f}{N} < 1\right),$$

or

$$Ro \left(\frac{l_0}{l}\right)^{2/3} \left(\frac{f}{N}\right)^{1/2} = Fr \left(\frac{l_0}{l}\right)^{2/3} \left(\frac{N}{f}\right)^{1/2} \ll 1 \left(\text{if } \frac{f}{N} > 1\right).$$

Therefore, at high Re, in addition to the above restrictions on the value of f/N, there is a restriction on the eddy size. In laboratory experiments and DNS for low- or moderate-Re flows, RDT is valid for low values of Fr or $Ro(f/N)^{1/2}$. On the other hand, at high Re, for the smaller scales of turbulence with $l/l_0 < Fr^{3/2}(f/N < 1)$ or $l/l_0 < Ro^{3/2}(f/N)^{3/4}(f/N > 1)$, RDT is not valid at small scales even if $Fr \ll 1(f/N < 1)$ or $Ro(f/N)^{1/2} \ll 1\,(f/N > 1)$ is satisfied.

It would be helpful to discuss the above criteria in more detail for the non-rotating case so that the comparison with the previous studies on time and length scales is clearer. The condition $Fr_l \ll 1$ is equivalent to the 'time' scale relation $l/u \gg N^{-1}$, which shows that the eddy overturning time is much larger than the buoyancy time scale, and the eddy is affected significantly by stratification. This can be also rewritten as a 'length' scale relation $l \gg (\epsilon/N^3)^{1/2} (\equiv L_o$, the Ozmidov scale or eddy overturning scale), under the assumption that the high-Reynolds-number relation $\epsilon = u(l)^3/l$ (=const) still holds even at scales for which the turbulence is affected by stratification. Then, if the energy-containing scale is larger than the Ozmidov scale ($l_0 \gg L_o$), we can expect that the energy-containing eddies are significantly affected by stratification. The equivalent condition $Fr \ll 1$, which can be derived by assuming $\epsilon = u_0^3/l_0$, is the condition for which linear theory gives a good approximation in the evaluation of the energies and the fluxes even when the small scales ($l < L_o$, i.e. $Fr_l > 1$) are affected by the nonlinear effects.

In previous studies and reviews on strongly stratified turbulence, Riley *et al.* (1981), Riley & Lelong (2000) and other authors who extended their results (e.g. Lilly 1983; McWilliams 1985; Embid & Majda 1996, 1998; Babin *et al.* 1997) have used the eddy overturning time l_0/u_H (u_H: horizontal velocity scale ($\sim u_0$)) as the time scale and also assumed the approximate hydrostatic balance $g\rho/\rho_0 = O((1/\rho_0)\partial p/\partial x_3)$ to estimate the density fluctuations ρ, and then derived the diagnostic equations for the vortex components. These scalings at the same time lead to the estimation of the vertical velocity as $u_3 = O(u_H Fr^2)$, which becomes very small compared to the horizontal velocity ($u_3/u_H = O(Fr^2) \ll 1$) at low Froude numbers ($Fr \ll 1$). In the limit of $Fr \to 0$ the governing equations reduce to the horizontally two-dimensional Navier–Stokes equations with vertical variability, i.e. with dependence on the vertical coordinate.

Another set of equations for the internal waves can also be derived by using a

different scaling for time ($t = O(N^{-1})$), which leads to the estimation of the vertical velocity as $u_3 = O(u_H)$, giving the same order as the horizontal velocity (e.g. Riley & Lelong 2000). In the limit of $Fr \to 0$ the internal wave equations become linear, showing that the wave components would be dominated by linear mechanisms when $Fr \ll 1$. These two equations for the vortex and wave components are quite important and useful to qualitatively understand the two major aspects of stratified turbulence, namely the waves and the vortices.

Since the vortex component equations have a nonlinear horizontal advection term even in the limit of $Fr \to 0$, nonlinear effects are important in the horizontal motion if the vortex components are dominant over the wave components. In a DNS for rotating stratified ($N = f$) turbulence (Bartello 1995), the energy spectra of the geostrophic (vortex) mode showed an inverse cascade just like two-dimensional turbulence, while those of the ageostrophic (wave) mode decayed at all scales.

On the other hand, the vertical velocity does not become so small in RDT and DNS which contain both the wave and vortex modes, even when $Fr \ll 1$. The key difference is the hydrostatic balance which is not assumed in RDT and DNS. If the hydrostatic balance holds and the vortex components dominate at the same time, the vertical velocity would be very small compared to the horizontal velocity when $Fr \ll 1$. Then, we may assume that RDT significantly overestimates the vertical velocity. However, Hanazaki & Hunt (1996) showed that the RDT gives better agreement with the DNS by Gerz & Yamazaki (1993) for stronger stratification, i.e. for smaller Fr, in the energy partition among the three kinetic energy components.

For initially isotropic turbulence without initial density perturbations, DNS by Métais & Herring (1989, cf. their figure 13) gives $PE/KE = 0.27$ at large times ($Nt \sim 300$, $(l_0/u_0)t \sim 30$) and at a small Froude number ($Fr \sim 0.1$), where PE is the turbulent potential energy associated with the density fluctuations and KE is the turbulent kinetic energy. Under these conditions, the scaling for the vortex component equations as described above gives $u_3^2/u_H^2 \sim Fr^4 = O(10^{-4})$, while RDT gives $PE/KE = 1/3$ ($Nt \to \infty$, Hanazaki & Hunt 1996). Since the potential energy PE and the wave mode energy E_W asymptote to almost equal values irrespective of the initial energy partitions (Métais & Herring 1989), we can put PE/KE equal to E_W/KE. Then, both the potential energy and the wave mode energy are predicted by RDT within errors of $< 20\%$. The vertical kinetic energy VKE is usually of the same order as the potential energy, and the vertical velocity also would not be very small. Then, the quantitative applicability of the scaling assumed to derive the vortex component equations becomes questionable at least in comparison with the DNS.

However, further quantitative comparisons with laboratory experiments, DNS and field observations are necessary to investigate the roles and the relative importance of the wave components and the vortex components. The hydrostatic balance might be better satisfied in the large-scale real atmosphere and ocean compared to the laboratory experiments and the DNS. If the hydrostatic balance holds, it may lead to a smaller vertical velocity. In the atmosphere and the ocean, it is still uncertain which components dominate since different observations give different results (Van Zandt 1982; Cho, Newell & Barrick 1999; see the introduction of Riley & Lelong 2000). Since RDT does not describe the nonlinear aspects of the vortex component equations, which may exist even when $Fr \ll 1$, there might arise a question about the applicability condition of RDT described above (i.e. $Fr \ll 1$), but the scaling argument used for the derivation of the vortex component equations is qualitative and not quantitative as discussed above; thus the scaling itself should be tested before quantitative discussion. Quantitative comparison of the solutions of the vortex

component equations with DNS or experiments has yet to be performed. To quantify the applicability of RDT, solution of the RDT equations in the Craya–Herring frame, where wave/vortex decomposition occurs automatically, is also desirable. Direct comparison with the DNS results will help clarify to what extent the wave mode is linear and the vortex mode is nonlinear. These subjects are now under investigation by the present author.

In the solutions of the horizontally two-dimensional Navier–Stokes equations with vertical variability, Majda & Grote (1997) have shown the vertical collapse of the columnar vortices into pancake structures due to viscous diffusion by the vertical shear. In their simulations, interactions between different horizontal wavenumber components are not included. More recently Galmiche & Hunt (2001) used RDT to show the initial formation of the vertical shear and density layers in decaying stratified turbulence. These results suggest that the nonlinear advection term in the horizontal momentum equation is important in upscale energy transfer to generate larger eddies, but the final decaying and layering processes might be the linear diffusive processes (Pearson & Linden 1983; Hanazaki & Hunt 1996).

3. Inviscid fluid

3.1. *Calculation of spectra*

We first consider inviscid fluid with $\nu = \kappa = 0$. In solving the RDT equations (2.6)–(2.7), we first write the equations in matrix form and calculate the eigenvalues and eigenvectors of the coefficient matrix. The four eigenvalues are 0 (degenerated) and $\pm \mathrm{i}a$, with

$$a = \frac{(N^2(k_1^2 + k_2^2) + f^2 k_3^2)^{1/2}}{k}. \tag{3.1}$$

Equation (3.1) is exactly the dispersion relation of the inertial gravity wave: the eigenvalue 0 corresponds to the non-propagating potential vorticity modes (geostrophic modes) and $\pm \mathrm{i}a$ correspond to the inertial gravity wave modes (Bartello 1995; Riley & Lelong 2000).

The two eigenvectors for eigenvalue 0 are

$$\boldsymbol{V}_1 = \begin{pmatrix} k_2 \\ -k_1 \\ 0 \\ fk_3 \end{pmatrix}, \tag{3.2}$$

and

$$\boldsymbol{V}_2 = \begin{pmatrix} 0 \\ 1 \\ f^2 k_2 k_3/(N^2(k_1^2 + k_2^2)) \\ -fk_1 k_3/(k_1^2 + k_2^2) \end{pmatrix}, \tag{3.3}$$

and the eivenvectors for eigenvalues $\pm \mathrm{i}a$ are

$$\boldsymbol{V}_3 = \begin{pmatrix} fk_2 + \mathrm{i}ak_1 \\ -fk_1 + \mathrm{i}ak_2 \\ -\mathrm{i}a(k_1^2 + k_2^2)/k_3 \\ -N^2(k_1^2 + k_2^2)/k_3 \end{pmatrix}, \tag{3.4}$$

and

$$\boldsymbol{V}_4 = \begin{pmatrix} fk_2 - \mathrm{i}ak_1 \\ -fk_1 - \mathrm{i}ak_2 \\ \mathrm{i}a(k_1^2 + k_2^2)/k_3 \\ -N^2(k_1^2 + k_2^2)/k_3 \end{pmatrix}. \tag{3.5}$$

Then, the RDT equations (2.6)–(2.7) give the following general solutions for $\hat{u}_i(t)$ $(i = 1, 2, 3)$ and $\hat{\rho}(t)$:

$$\hat{\rho} = \hat{\rho}_0 \left[\cos at + \frac{f^2k_3^2}{a^2k^2}(1 - \cos at)\right] + \frac{N^2}{a}\hat{u}_{30} \sin at + \frac{fN^2k_3}{a^2k^2}(1 - \cos at)(k_2\hat{u}_{10} - k_1\hat{u}_{20}), \tag{3.6}$$

$$\begin{aligned} \hat{u}_1 = {} & \hat{u}_{10}\left[1 + \frac{f^2k_3^2}{a^2k^2}(\cos at - 1) - \frac{fk_1k_2k_3^2}{ak^2(k_1^2 + k_2^2)} \sin at\right] + \hat{u}_{20}\frac{fk_1^2k_3^2}{ak^2(k_1^2 + k_2^2)} \sin at \\ & + \hat{u}_{30}\left[\frac{N^2k_1k_3}{a^2k^2}(1 - \cos at) - \frac{fk_2k_3}{a(k_1^2 + k_2^2)} \sin at\right] \\ & + \hat{\rho}_0\left[\frac{fk_2k_3}{a^2k^2}(1 - \cos at) + \frac{k_1k_3}{ak^2} \sin at\right], \end{aligned} \tag{3.7}$$

$$\begin{aligned} \hat{u}_2 = {} & -\hat{u}_{10}\frac{fk_2^2k_3^2}{ak^2(k_1^2 + k_2^2)} \sin at + \hat{u}_{20}\left[1 + \frac{f^2k_3^2}{a^2k^2}(\cos at - 1) + \frac{fk_1k_2k_3^2}{ak^2(k_1^2 + k_2^2)} \sin at\right] \\ & + \hat{u}_{30}\left[\frac{N^2k_2k_3}{a^2k^2}(1 - \cos at) + \frac{fk_1k_3}{a(k_1^2 + k_2^2)} \sin at\right] \\ & + \hat{\rho}_0\left[\frac{fk_1k_3}{a^2k^2}(\cos at - 1) + \frac{k_2k_3}{ak^2} \sin at\right], \end{aligned} \tag{3.8}$$

$$\hat{u}_3(t) = \hat{u}_{30} \cos at + \frac{fk_3}{ak^2}(k_2\hat{u}_{10} - k_1\hat{u}_{20}) \sin at - \frac{k_1^2 + k_2^2}{ak^2}\hat{\rho}_0 \sin at, \tag{3.9}$$

where k denotes $|\boldsymbol{k}|$, the subscript 0 denotes the initial values, and we have used the incompressibility condition $k_i\hat{u}_{i0} = 0$ to simplify the expressions. The solutions for $\hat{\rho}$ and $\hat{u}_3$ without initial density fluctuations ($\hat{\rho}_0 = 0$) have been obtained by Iida & Nagano (1999).

Then we can calculate all the three-dimensional spectrum functions. In this study we assume that the initial density fluxes are zero, i.e.

$$\Phi_{\rho i}(\boldsymbol{k}, 0) = \tfrac{1}{2}\overline{\hat{\rho}_0^*\hat{u}_{30} + \hat{\rho}_0\hat{u}_{30}^*} = 0 \quad (i = 1, 2, 3). \tag{3.10}$$

The results are

$$\begin{aligned} \Phi_{\rho 3}(\boldsymbol{k}, t) = {} & \tfrac{1}{2}\overline{\hat{\rho}^*\hat{u}_3 + \hat{\rho}\hat{u}_3^*} \\ = {} & -\frac{k_1^2 + k_2^2}{k^2a}\left[\cos at + \frac{f^2k_3^2}{k^2a^2}(1 - \cos at)\right] \sin at\Phi_{\rho\rho}(\boldsymbol{k}, 0) + \frac{N^2}{2a}\Phi_{33}(\boldsymbol{k}, 0) \sin 2at \\ & + \frac{f^2N^2k_3^2}{a^3k^4}(k_2^2\Phi_{11}(\boldsymbol{k}, 0) + k_1^2\Phi_{22}(\boldsymbol{k}, 0) - 2k_1k_2\Phi_{12}(\boldsymbol{k}, 0))(1 - \cos at) \sin at \\ & + \frac{fN^2k_3}{a^2k^2}(k_2\Phi_{13}(\boldsymbol{k}, 0) - k_1\Phi_{23}(\boldsymbol{k}, 0))(\cos at - \cos 2at), \end{aligned} \tag{3.11}$$

$$\Phi_{11}(\boldsymbol{k},t) = \Phi_{11}(\boldsymbol{k},0)\left[1+\frac{f^2k_3^2}{a^2k^2}(\cos at-1)-\frac{fk_1k_2k_3^2}{ak^2(k_1^2+k_2^2)}\sin at\right]^2$$
$$+2\Phi_{12}(\boldsymbol{k},0)\left[1+\frac{f^2k_3^2}{a^2k^2}(\cos at-1)-\frac{fk_1k_2k_3^2}{ak^2(k_1^2+k_2^2)}\sin at\right]\frac{fk_1^2k_3^2}{ak^2(k_1^2+k_2^2)}\sin at$$
$$+2\Phi_{13}(\boldsymbol{k},0)\left[1+\frac{f^2k_3^2}{a^2k^2}(\cos at-1)-\frac{fk_1k_2k_3^2}{ak^2(k_1^2+k_2^2)}\sin at\right]$$
$$\times\left[\frac{N^2k_1k_3}{a^2k^2}(1-\cos at)-\frac{fk_2k_3}{a(k_1^2+k_2^2)}\sin at\right]$$
$$+\Phi_{22}(\boldsymbol{k},0)\frac{f^2k_1^4k_3^4}{a^2k^4(k_1^2+k_2^2)^2}\sin^2 at$$
$$+2\Phi_{23}(\boldsymbol{k},0)\frac{fk_1^2k_3^2}{ak^2(k_1^2+k_2^2)}\sin at\left[\frac{N^2k_1k_3}{a^2k^2}(1-\cos at)-\frac{fk_2k_3}{a(k_1^2+k_2^2)}\sin at\right]$$
$$+\Phi_{33}(\boldsymbol{k},0)\left[\frac{N^2k_1k_3}{a^2k^2}(1-\cos at)-\frac{fk_2k_3}{a(k_1^2+k_2^2)}\sin at\right]^2$$
$$+\Phi_{\rho\rho}(\boldsymbol{k},0)\left[\frac{fk_2k_3}{a^2k^2}(1-\cos at)+\frac{k_1k_3}{ak^2}\sin at\right]^2, \tag{3.12}$$

$$\Phi_{33}(\boldsymbol{k},t) = \Phi_{33}(\boldsymbol{k},0)\cos^2 at+\frac{f^2k_3^2}{a^2k^4}\sin^2 at(k_2^2\Phi_{11}(\boldsymbol{k},0)+k_1^2\Phi_{22}(\boldsymbol{k},0)-2k_1k_2\Phi_{12}(\boldsymbol{k},0))$$
$$+\frac{(k_1^2+k_2^2)^2}{a^2k^4}\sin^2 at\Phi_{\rho\rho}(\boldsymbol{k},0)$$
$$+\frac{2fk_3}{ak^2}\sin at\cos at\,(k_2\Phi_{13}(\boldsymbol{k},0)-k_1\Phi_{23}(\boldsymbol{k},0)), \tag{3.13}$$

$$\Phi_{\rho\rho}(\boldsymbol{k},t) = \Phi_{\rho\rho}(\boldsymbol{k},0)\left[\cos at+\frac{f^2k_3^2}{a^2k^2}(1-\cos at)\right]^2+\frac{N^4}{a^2}\sin^2 at\Phi_{33}(\boldsymbol{k},0)$$
$$+\frac{f^2N^4k_3^2}{a^4k^4}(1-\cos at)^2(k_2^2\Phi_{11}(\boldsymbol{k},0)+k_1^2\Phi_{22}(\boldsymbol{k},0)-2k_1k_2\Phi_{12}(\boldsymbol{k},0))$$
$$+\frac{2fN^4k_3}{a^3k^2}\sin at(1-\cos at)\,(k_2\Phi_{13}(\boldsymbol{k},0)-k_1\Phi_{23}(\boldsymbol{k},0)), \tag{3.14}$$

where we have used $k_i\Phi_{ij} = k_j\Phi_{ij} = 0$ derived from the incompressibility condition $k_i\hat{u}_{i0} = 0$.

It would be useful to mention here general relations among the three-dimensional spectra directly derived from (2.6) and (2.7), applicable to fluid with viscosity and diffusion:

$$\left(\frac{\mathrm{d}}{\mathrm{d}t}+2\nu k^2\right)\sum_i\Phi_{ii} = -2\Phi_{\rho 3}, \tag{3.15}$$

$$\left(\frac{\mathrm{d}}{\mathrm{d}t} + 2\kappa k^2\right) \Phi_{\rho\rho} = 2N^2 \Phi_{\rho 3}. \tag{3.16}$$

These relations are the same as in flow with pure stratification ($N \neq 0, f = 0$), and when integrated in spectral space, they show that the exchange between the total kinetic energy and the potential energy is achieved exclusively by the vertical density flux $\overline{\rho u_3}$ even when there is a system rotation.

There are several more complicated relations which include rotation effects (f) explicitly, i.e.

$$\left(\frac{\mathrm{d}}{\mathrm{d}t} + 2\nu k^2\right) \Phi_{ij} = \left[\left(\frac{k_i k_n}{k^2} - \delta_{in}\right) \Phi_{lj} + \left(\frac{k_j k_n}{k^2} - \delta_{jn}\right) \Phi_{li}\right] \epsilon_{n3l} f + \left(\frac{k_i k_3}{k^2} - \delta_{i3}\right) \Phi_{\rho j} + \left(\frac{k_j k_3}{k^2} - \delta_{j3}\right) \Phi_{\rho i}, \tag{3.17}$$

$$\left(\frac{\mathrm{d}}{\mathrm{d}t} + (\nu + \kappa) k^2\right) \Phi_{\rho i} = \left(\frac{k_i k_j}{k^2} - \delta_{ij}\right) \Phi_{\rho l} \epsilon_{j3l} f + \left(\frac{k_i k_3}{k^2} - \delta_{i3}\right) \Phi_{\rho\rho} + N^2 \Phi_{i3}. \tag{3.18}$$

When $f = 0$, these relations reduce to the non-rotating results by Hanazaki & Hunt (1996).

4. Initially isotropic turbulence

4.1. *Initial conditions*

We consider turbulence under stable stratification ($N^2 > 0$) in this section and § 5. In addition, since the turbulence is usually initially isotropic in laboratory experiments for grid turbulence and in most of the DNS, we first consider initially isotropic turbulence in this section. The initial conditions for the three-dimensional spectra are given by

$$\Phi_{ij}(\boldsymbol{k}, 0) = \frac{E(k)}{4\pi k^2} \left(\delta_{ij} - \frac{k_i k_j}{k^2}\right) \tag{4.1}$$

and

$$\Phi_{\rho\rho}(\boldsymbol{k}, 0) = \frac{S(k)}{4\pi k^2} 2N^2, \tag{4.2}$$

where

$$KE_0 = \int_0^\infty E(k)\, \mathrm{d}k \tag{4.3}$$

and

$$PE_0 = \frac{1}{2N^2} \int \Phi_{\rho\rho}(\boldsymbol{k}, 0)\, \mathrm{d}\boldsymbol{k} = \int_0^\infty S(k)\, \mathrm{d}k, \tag{4.4}$$

are the initial turbulent kinetic and potential energy.

We now write the wavenumber vector in spherical coordinates as

$$k_1 = k \sin\theta \cos\phi, \quad k_2 = k \sin\theta \sin\phi, \quad k_3 = k \cos\theta, \tag{4.5}$$

so that

$$k^2 = k_1^2 + k_2^2 + k_3^2, \tag{4.6}$$

and

$$\sin\theta = \frac{(k_1^2 + k_2^2)^{1/2}}{k} = \frac{k_H}{k}, \tag{4.7}$$

where k_H is the horizontal wavenumber defined by

$$k_H = (k_1^2 + k_2^2)^{1/2}. \tag{4.8}$$

The frequency a defined by (3.1) can be rewritten as

$$a^2 = f^2\cos^2\theta + N^2\sin^2\theta. \tag{4.9}$$

4.2. *Variances and covariances*

Using (3.11), we obtain the vertical density flux as

$$\begin{aligned}\overline{\rho u_3}(t) &= \int \Phi_{\rho 3}(\boldsymbol{k}, t) 2\pi k^2 \,\mathrm{d}k \sin\theta \,\mathrm{d}\theta \\ &= \frac{N^2}{2} E_0^{(C)} \int_0^\pi \mathrm{d}\theta \frac{\sin^3\theta}{a^3} \sin at (N^2\sin^2\theta\cos at + f^2\cos^2\theta),\end{aligned} \tag{4.10}$$

where $E_0^{(C)} = KE_0 - 2PE_0$ is the complementary energy which represents the deviation from the equilibrium state of turbulence.

Other variances and covariances can be calculated similarly and the results are

$$\begin{aligned}\overline{u_1^2}(t) = \overline{u_2^2}(t) &= \tfrac{2}{3}KE_0 + \frac{N^2}{8}E_0^{(C)} \int_0^\pi \mathrm{d}\theta \frac{\sin^3\theta\cos^2\theta}{a^4} \\ &\quad \times (4f^2\cos^2\theta(\cos at - 1) + (f^2 - N^2)\sin^2\theta(1 - \cos 2at)),\end{aligned} \tag{4.11}$$

$$\overline{u_3^2}(t) = \tfrac{2}{3}KE_0 - \frac{N^2}{2}E_0^{(C)} \int_0^\pi \mathrm{d}\theta \frac{\sin^5\theta}{a^2}\sin^2 at, \tag{4.12}$$

and

$$\overline{\rho^2}(t) = 2N^2 PE_0 + \frac{N^4}{4}E_0^{(C)} \int_0^\pi \mathrm{d}\theta \frac{\sin^3\theta}{a^4} \left(N^2\sin^2\theta(1 - \cos 2at) + 4f^2\cos^2\theta(1 - \cos at)\right). \tag{4.13}$$

We note that the sign of $E_0^{(C)}$ determines the direction of the oscillation. In other words, the initial partition of energy between the kinetic and potential energy, $KE_0/PE_0 < 2$ or > 2, determines the subsequent direction of the vertical density (heat) transport at a specific time.

In the case of pure rotation ($N = 0, f \neq 0$), energy partition does not change with time and $\overline{u_1^2}(t) = \overline{u_2^2}(t) = \overline{u_3^2}(t) = \frac{2}{3}KE_0$ holds at all times. This recovers the DNS results for initially isotropic rotating turbulence which retained initial isotropy (Bardina *et al.* 1985) and also recovers the results from linear theory (Greenspan 1968; Cambon & Jacquin 1989).

On the other hand, in the case of pure stratification ($f = 0, N \neq 0$), the above results reduce to those by Hanazaki & Hunt (1996).

We note finally that total turbulence energy is conserved in inviscid fluid, i.e.

$$\begin{aligned}KE(t) + PE(t) &= \tfrac{1}{2}(\overline{u_1^2} + \overline{u_2^2} + \overline{u_3^2}) + \frac{1}{2N^2}\overline{\rho^2} \\ &= KE_0 + PE_0.\end{aligned} \tag{4.14}$$

4.3. *Short-time approximations*

When both $Nt \ll 1$ and $ft \ll 1$ are satisfied, we obtain the short-time approximations as

$$\overline{\rho u_3}(t) = N^2 E_0^{(C)} t(\tfrac{2}{3} - \tfrac{16}{45}(Nt)^2 - \tfrac{1}{45}(ft)^2 + O(t^4)),$$

$$\overline{u_1^2}(t) = \tfrac{2}{3}KE_0 - \tfrac{1}{4}E_0^{(C)}(Nt)^2(\tfrac{4}{15} - \tfrac{16}{315}(Nt)^2 + \tfrac{1}{35}(ft)^2 + O(t^4)),$$

$$\overline{u_3^2}(t) = \tfrac{2}{3}KE_0 + E_0^{(C)}(Nt)^2(-\tfrac{8}{15} + \tfrac{16}{105}(Nt)^2 + \tfrac{8}{315}(ft)^2 + O(t^4)),$$

$$\overline{\rho^2}(t) = 2N^2 PE_0 + E_0^{(C)} N^2 (Nt)^2(\tfrac{2}{3} - \tfrac{8}{45}(Nt)^2 - \tfrac{1}{90}(ft)^2 + O(t^4)). \tag{4.15}$$

It is of interest here to note that the rotation effects represented by f appear only in higher-order corrections of $O(t^3)$ or $O(t^4)$ and the dominant terms of the initial time development are determined only by N. This means that even with the Coriolis effects, the initial time development of turbulence is governed essentially by stratification. If $f \gg N$, the higher-order terms which contain f can become large. However, in the usual geophysical contexts, the rotation period of the Earth is much larger than the buoyancy period ($f \ll N$). Therefore, at least in geophysical applications, the effect of f would be negligible initially. The effects of rotation f becomes apparent at later times.

The initial normalized vertical density flux $\overline{\rho u_3}/(\overline{\rho^2}^{1/2}\overline{u_3^2}^{1/2})$ $(Nt, ft \to 0)$ obtained from (4.15) is identical to that for non-rotating stratified turbulence. If there is no initial kinetic energy ($KE_0 = 0$), we obtain

$$\frac{\overline{\rho u_3}}{\overline{\rho^2}^{1/2}\overline{u_3^2}^{1/2}}(Nt, ft \to 0) = -(\tfrac{5}{6})^{1/2} = -0.913. \tag{4.16}$$

This agrees with the results of DNS (Gerz & Yamazaki 1993) and RDT (Hanazaki & Hunt 1996) for non-rotating stratified fluids. If there is no initial potential energy ($PE_0 = 0$), we obtain

$$\frac{\overline{\rho u_3}}{\overline{\rho^2}^{1/2}\overline{u_3^2}^{1/2}}(Nt, ft \to 0) = 1, \tag{4.17}$$

again in agreement with the non-rotating results (Hanazaki & Hunt 1996).

If we substitue $f = 0$ into (4.15), short-time approximations for the non-rotating stratified turbulence (Hunt *et al.* 1988; Hanazaki & Hunt 1996) could of course be recovered.

4.4. *Long-time asymptotics*

4.4.1. *General case of $N \neq f$*

When the Brunt–Väisälä frequency and the Coriolis parameter are not equal ($N \neq f$), the dispersion relation of the gravity wave, i.e. (3.1) or (4.9), shows that a depends on θ. In this case, examination of the integrals (4.10)–(4.13) shows that, at large times ($Nt \gg 1$ or $ft \gg 1$), the most slowly oscillating components with θ in the integrand, the component which satisfies $\partial a/\partial\theta = 0$, contribute most to the integral. This is the essence of the method of stationary phase and it can be applied to the present case as has been done for pure stratification (Hanazaki & Hunt 1996). We should keep in mind that this method gives good approximations even when the time is not very large, i.e. even for $Nt, ft = O(1)$ (e.g. Hinch 1991). Since the stationary phase $\theta_0 = \pi/2$ satisfies $\cos\theta_0 = 0$, the rotation effects in the integrand

cannot contribute significantly to the integral in the long-time limit, since the Coriolis parameter f appears only in the form of $f\cos\theta$, i.e. it is always coupled with $\cos\theta(=0)$. The angle of stationary phase $\theta_0 = \pi/2$ gives the horizontal wavenumber vector ($k_3 = k\cos\theta_0 = 0$) and $a = N$, which means that the pure buoyant oscillation with frequency N in the vertical plane contributes to the unsteadiness of the variances and the covariances even in rotating fluids.

The long-time behaviours become

$$\overline{\rho u_3}(t) = \frac{N}{4}E_0^{(C)}\left(\frac{\pi N}{t|N^2-f^2|}\right)^{1/2}\sin\left(2Nt \pm \frac{\pi}{4}\right), \tag{4.18}$$

$$\overline{u_1^2}(t) = \overline{u_2^2}(t) = \tfrac{2}{3}KE_0 + E_0^{(C)}\left[\frac{N^2(23f^2-2N^2)}{24(f^2-N^2)^2} - \frac{N^2f^2(3f^2+4N^2)}{8(f^2-N^2)^3}I_A\right], \tag{4.19}$$

$$\overline{u_3^2}(t) = \tfrac{2}{3}KE_0 + E_0^{(C)}\left[\frac{N^2(5f^2-2N^2)}{6(f^2-N^2)^2} - \frac{N^2f^4}{2(f^2-N^2)^3}I_A\right] + \tfrac{1}{4}E_0^{(C)}\left(\frac{\pi N}{t|N^2-f^2|}\right)^{1/2}\cos\left(2Nt \pm \frac{\pi}{4}\right), \tag{4.20}$$

$$\overline{\rho^2}(t) = 2N^2PE_0 + E_0^{(C)}\left[-\frac{N^4(11f^2-2N^2)}{4(f^2-N^2)^2} + \frac{N^4f^2(5f^2+4N^2)}{4(f^2-N^2)^3}I_A\right] - \frac{N^2}{4}E_0^{(C)}\left(\frac{\pi N}{t|N^2-f^2|}\right)^{1/2}\cos\left(2Nt \pm \frac{\pi}{4}\right), \tag{4.21}$$

where

$$I_A = \int_0^1 \frac{\mathrm{d}x}{x^2 + N^2/(f^2-N^2)} = \frac{(f^2-N^2)^{1/2}}{N}\tan^{-1}\frac{(f^2-N^2)^{1/2}}{N}(f > N)$$

or

$$= \frac{(N^2-f^2)^{1/2}}{N}\log\frac{N-(N^2-f^2)^{1/2}}{f}(f < N), \tag{4.22}$$

and the sign $\pm$ represents $+$ when $f > N$, and $-$ when $f < N$.

As discussed above, vertically uniform components ($k_3 = 0$) do not contribute to the vertical density flux given by (4.18), and the vertical density transport is maintained essentially by stratification even when rotation exists. The oscillation period $2\pi/2N$ is the same as in the case of pure stratification (Hanazaki & Hunt 1996) and the flux amplitude is modified only by the factor of $(N^2/|N^2-f^2|)^{1/2}$ compared to the non-rotating result. This is nearly equal to 1 when $f \ll N$, showing that rotation does not contribute to the unsteady components of the vertical density (heat) flux in the atmosphere and ocean, where typical values of f and N are $f \approx 7.3\times10^{-5}\,\mathrm{s}^{-1}$ and $N \approx 10^{-2}\,\mathrm{s}^{-1}$.

An important effect of rotation on the unsteadiness is that there is a 'phase shift' ($\pm\pi/4$) depending on the relative values of f and N, i.e. whether $f > N$ or $f < N$. This explains the apparent difference in the oscillation 'period' between the non-rotating

results ($N > f = 0$) and other rapidly rotating results ($f > N$) observed in DNS (cf. § 9, figure 1).

We note that, if $f \ll N$ is satisfied, the energy ratio $ER = PE/VKE$ of the potential energy to the vertical kinetic energy becomes approximately

$$ER = \frac{\overline{\rho^2}/(2N^2)}{\overline{u_3^2}/2} \to \tfrac{3}{2}(Nt \gg 1), \tag{4.23}$$

as in the case of pure stratification (Hanazaki & Hunt 1996), although weak dependence on f might be observed when $f \neq 0$. This value roughly agrees with the observed value of $ER = 1.0 \pm 0.3$ in the atmosphere (Nieuwstadt 1984; Hunt, Kaimal & Gaynor 1985).

It is clear from (4.19)–(4.21) that the final 'steady' values of the energy components depend on the ratio of the Coriolis parameter f to the Brunt–Väisälä frequency N, i.e. f/N, in addition to the initial kinetic energy KE_0 and the initial potential energy PE_0. Bartello (1995) performed DNS for decaying stratified rotating turbulence under the conditions $N = 5.3$, $f = 8.7$, $PE_0 = 0$ and $Pr = 1$. Although hyperviscosity was used and no information on the initial spectral forms were given in that paper, we can calculate long-time asymptotics of the ratio of kinetic energy to the potential energy KE/PE ($t \to \infty$) by inviscid RDT as long as $Pr = 1$ holds, since the viscosity/diffusion effects are cancelled out in the analytical expression of KE/PE, as is clear from the formulations described later in § 6. Substituting $f/N = 1.64$ and $PE_0 = 0$ into (4.19)–(4.21), we obtain the long-time limit values as $\overline{u_1^2} = \overline{u_2^2} = 0.54KE_0$, $\overline{u_3^2} = 0.44KE_0$ and $PE = (1/2N^2)\overline{\rho^2} = 0.24KE_0$. Then we obtain $KE/PE(t \to \infty) = 3.2$ (and $ER(t \to \infty) = 1.1$), in good agreement with the DNS results which gave $KE/PE(t \to \infty) \sim 3.0$ (figure 5 of Bartello 1995).

4.4.2. *Special case of $N = f$*

As is clear from the above expressions (4.18)–(4.21), the method of steepest descents cannot be applied when $N = f$. In this case the dispersion relation for the inertial gravity wave gives $a = N = f$, showing that the group velocity of the wave is zero and the wave energy does not propagate. However, the exact solution becomes much simpler and the integration can be done exactly to give the variances and the covariances at an arbitrary time. The results are

$$\overline{\rho u_3}(t) = \tfrac{2}{15}NE_0^{(C)}(\sin Nt + 2\sin 2Nt), \tag{4.24}$$

$$\overline{u_1^2}(t) = \overline{u_2^2}(t) = \tfrac{2}{3}KE_0 + \tfrac{2}{15}E_0^{(C)}(\cos Nt - 1), \tag{4.25}$$

$$\overline{u_3^2}(t) = \tfrac{2}{3}KE_0 + \tfrac{4}{15}E_0^{(C)}(\cos 2Nt - 1), \tag{4.26}$$

and

$$\overline{\rho^2}(t) = 2N^2PE_0 + \tfrac{4}{15}N^2E_0^{(C)}(2 - \cos Nt - \cos 2Nt). \tag{4.27}$$

We note that, when $N = f$, oscillations in the variances and the covariances do not decay with time in contrast to the case of $N \neq f$.† In this case, $a(= N = f)$ is independent of θ so that all the spectral components oscillate with the same period $2\pi/N(= 2\pi/f)$ independent of the direction of the wavenumber, as do the three-dimensional spectra. Thus there is no phase difference which leads to the inviscid

† After submission of this paper we noticed that similar results have been obtained by Kaneda (2000) for diffusion problems in stratified rotating turbulence.

decay of oscillations (Hanazaki & Hunt 1996; Kaneda & Ishida 2000), and the energies never reach constant values in inviscid fluid.

It is also of interest to note that $\overline{u_1^2}(=\overline{u_2^2})$ contains only the $\cos Nt$ component and not $\sin 2Nt$ or $\cos 2Nt$, showing that the horizontal kinetic energy oscillates slower than the vertical kinetic energy and the potential energy. As will be discussed later, the slow oscillation with frequency N has been observed in DNS (see §9, figure 2) when the initial turbulence is anisotropic and $N = f$ is satisfied. It is not the result of the initial anisotropy but because $N = f$. The results for $\overline{u_1^2}$ $(=\overline{u_2^2})$ and $\overline{\rho^2}$ show that energy exchange occurs at lower frequency N exclusively between the horizontal kinetic energy and the potential energy, without any explicit participation of the vertical kinetic energy. On the other hand, the high-frequency energy exchange at frequency $2N$, as in the general case of $f \neq N$, occurs between the vertical kinetic energy and the potential energy.

5. Initially axisymmetric turbulence

5.1. *Initial conditions*

Since pure rotation does not affect the horizontal and vertical kinetic energy partition for initially isotropic turbulence, it is of interest to see what occurs for initially axisymmetric turbulence in stratified rotating fluids. If we assume initially axisymmetric and purely horizontal turbulence which satisfies $\overline{u_1^2}(0) = \overline{u_2^2}(0)(= KE_0)$ and $\overline{u_3^2}(0) = 0$, the initial three-dimensional spectra for the Reynolds stresses with zero helicity are (Herring 1974; Schumann & Patterson 1978)

$$\Phi_{11}(\boldsymbol{k},0) = \frac{E(k)}{2\pi k^2}\sin^2\phi, \tag{5.1}$$

$$\Phi_{12}(\boldsymbol{k},0) = -\frac{E(k)}{2\pi k^2}\sin\phi\cos\phi, \tag{5.2}$$

$$\Phi_{22}(\boldsymbol{k},0) = \frac{E(k)}{2\pi k^2}\cos^2\phi, \tag{5.3}$$

and

$$\Phi_{13}(\boldsymbol{k},0) = \Phi_{23}(\boldsymbol{k},0) = \Phi_{33}(\boldsymbol{k},0) = 0. \tag{5.4}$$

The initial density perturbation spectrum is

$$\Phi_{\rho\rho}(\boldsymbol{k},0) = \frac{S(k)}{4\pi k^2}2N^2. \tag{5.5}$$

5.2. *Energies*

Using (3.12)–(3.14), the three-dimensional spectra can be obtained and the energy components are

$$\overline{u_1^2}(t) = \overline{u_2^2}(t) = \tfrac{1}{2}KE_0\int_0^\pi \mathrm{d}\theta\frac{\sin\theta}{a^4}\left[\left(a^2 + f^2\cos^2\theta(\cos at - 1)\right)^2 + a^2f^2\cos^4\theta\sin^2 at\right]$$
$$+ \frac{N^2}{2}PE_0\int_0^\pi \mathrm{d}\theta\frac{\sin^3\theta\cos^2\theta}{a^4}\left[f^2(1-\cos at)^2 + a^2\sin^2 at\right]^2, \tag{5.6}$$

$$\overline{u_3^2}(t) = f^2KE_0\int_0^\pi \mathrm{d}\theta\frac{\sin^3\theta\cos^2\theta}{a^2}\sin^2 at + N^2PE_0\int_0^\pi \mathrm{d}\theta\frac{\sin^5\theta}{a^2}\sin^2 at, \tag{5.7}$$

$$\overline{\rho^2}(t) = f^2N^4KE_0\int_0^\pi \mathrm{d}\theta \frac{\sin^3\theta\cos^2\theta}{a^4}(1-\cos at)^2$$

$$+ N^2PE_0\int_0^\pi \mathrm{d}\theta\left[\cos at + \frac{f^2\cos^2\theta}{a^2}(1-\cos at)\right]^2. \tag{5.8}$$

In contrast to initially isotropic turbulence, even without stratification ($N = 0$), pure rotation modifies the partition between the horizontal and vertical kinetic energies. When $N = 0$, the integration can be done exactly and the results will be given in § 5.3.2.

5.3. *Long-time asymptotics*

5.3.1. *General case of $N \neq f$*

In the general case of $N \neq f$ the long-time approximations give

$$\overline{u_1^2}(t) = \overline{u_2^2}(t) = KE_0\left[\frac{2}{3} + \frac{N^2(17f^2+4N^2)}{12(f^2-N^2)^2} - \frac{f^2N^2(f^2+6N^2)}{4(f^2-N^2)^3}I_A\right]$$

$$+ PE_0\left[\frac{N^2(-23f^2+2N^2)}{12(f^2-N^2)^2} + \frac{f^2N^2(3f^2+4N^2)}{4(f^2-N^2)^3}I_A\right], \tag{5.9}$$

$$\overline{u_3^2}(t) = \tfrac{2}{3}KE_0 + (KE_0 - PE_0)\frac{N^2(5f^2-2N^2)}{3(f^2-N^2)^2} - (KE_0-PE_0)\frac{f^4N^2}{(f^2-N^2)^3}I_A$$

$$- \tfrac{1}{2}PE_0\left(\frac{\pi N}{t|N^2-f^2|}\right)^{1/2}\cos\left(2Nt \pm \frac{\pi}{4}\right), \tag{5.10}$$

and

$$\overline{\rho^2}(t) = \tfrac{3}{2}KE_0f^2N^4\left[-\frac{3}{(f^2-N^2)^2} + \frac{f^2+2N^2}{(f^2-N^2)^3}I_A\right]$$

$$+ PE_0\frac{N^2}{2}\left[\frac{4f^4+3f^2N^2+2N^4}{(f^2-N^2)^2} - \frac{f^2N^2(5f^2+4N^2)}{(f^2-N^2)^3}I_A\right]$$

$$+ PE_0\frac{N^2}{2}\left(\frac{\pi N}{t|N^2-f^2|}\right)^{1/2}\cos\left(2Nt \pm \frac{\pi}{4}\right) \tag{5.11}$$

where I_A is again given by (4.22).

We note in (5.9)–(5.11) that the final steady values of the energy components depend on the ratio of the Coriolis parameter f to the Brunt–Väisälä frequency N, i.e. f/N, in addition to KE_0 and PE_0, as in the initially isotropic conditions. We also note that, if stratification exists ($N \neq 0$), the final energy distribution is generally anisotropic.

5.3.2. *Special case of pure rotation ($N = 0$)*

In the case of pure rotation ($N = 0$), the above expressions give the long-time limit ($t \to \infty$) values as

$$\left.\begin{aligned}\overline{u_1^2}(t) &= \overline{u_2^2}(t) = \tfrac{2}{3}KE_0,\\ \overline{u_3^2}(t) &= \tfrac{2}{3}KE_0,\\ \overline{\rho^2}(t) &= 0,\end{aligned}\right\} \tag{5.12}$$

showing the return to exact isotropy by the linear mechanism. However, the asymptotics obtained by the method of stationary phase cannot capture the time development, which would decay faster than $O(t^{-1/2})$.

The integrals in (5.6)–(5.8) can be calculated exactly. As noted by Mansour, Shih & Reynolds (1991), the integrals of the form

$$I_n \equiv \int_0^\pi \mathrm{d}\theta \sin\theta \cos^n\theta \cos(c\cos\theta) = \int_{-1}^1 \mathrm{d}x x^n \cos(cx), \tag{5.13}$$

where $c = 2ft$, can be calculated from the partial integral and the exact results are

$$I_0 = 2\frac{\sin c}{c}, \tag{5.14}$$

and

$$I_2 = 2\frac{\sin c}{c} + 4\frac{\cos c}{c^2} - 4\frac{\sin c}{c^3}. \tag{5.15}$$

In general $I_n (n = 2, 4, 6, \ldots)$ can be calculated by the recursive relation

$$I_n = \frac{2}{c}\sin c + \frac{2n}{c^2}\cos c - \frac{n(n-1)}{c^2} I_{n-2}. \tag{5.16}$$

The value of I_4 is given in Mansour *et al.* (1991), and values of I_n for larger n might become necessary for some specific initial conditions used, but we need only I_0 and I_2 here. Then, (5.6) and (5.7) become

$$\left.\begin{aligned} \overline{u_1^2}(t) = \overline{u_2^2}(t) &= \tfrac{2}{3}KE_0 - KE_0\left(\frac{\cos 2ft}{(2ft)^2} - \frac{\sin 2ft}{(2ft)^3}\right), \\ \overline{u_3^2}(t) &= \tfrac{2}{3}KE_0 + 2KE_0\left(\frac{\cos 2ft}{(2ft)^2} - \frac{\sin 2ft}{(2ft)^3}\right). \end{aligned}\right\} \tag{5.17}$$

These allow decaying oscillations of the anisotropy tensor b_{ij} similar to those observed in the DNS and RDT by Mansour *et al.* (1991) for initially anisotropic rotating turbulence. Note that the leading-order time-dependent terms have decaying oscillations whose amplitude decays like $\propto t^{-2}$, much faster than $\propto t^{-1/2}$ as observed in (5.10) for stratified rotating turbulence. In the study of Mansour *et al.* (1991), the anisotropy tensor bj decayed like $\propto t^{-1}$, which is slower than ours. The difference is attributable to the different initial conditions, since their anisotropic initial condition (Shih, Reynolds & Mansour 1990) did not assume axisymmetry of the turbulence.

We have calculated the higher-order asymptotics for the general case of $N \neq f$ to $O(t^{-3/2})$ using higher-order steepest descents (Whitham 1974). The results give a term proportional to

$$\frac{\pi^{1/2}}{2N^{1/2}(|N^2 - f^2|t)^{3/2}} \sin\left(2Nt \pm \frac{\pi}{4}\right), \tag{5.18}$$

and terms with frequency $2f$ do not appear even at this higher order, since the components with horizontal wavenumber ($\theta = \pi/2$) become dominant as in the leading-order term. These results show that the characteristics of the time development in pure rotating turbulence have been changed significantly by stratification. This corresponds to the fact that the wave character changes from inertial waves to gravity waves.

It is of interest to note that the final isotropy of pure rotating turbulence is independent of whether the initial turbulence was three-dimensionally isotropic or

axisymmetric. Final anisotropy is purely the result of stratification. Since arbitrary axisymmetric turbulence can be composed of the superposition of three-dimensional isotropic turbulence and purely horizontal turbulence (Herring 1974), we can conclude that any rotation (unstratified) turbulence initially axisymmetric around the rotation axis finally returns to isotropy. In numerical solutions of RDT equations with viscosity, Cambon & Jacquin (1989) showed that $\overline{u_3^2}/\overline{u_1^2}$ tends to 0.9 for initial axisymmetric expansion and to 1.2 for initial axisymmetric contraction. These long-time asymptotic values show approximate return to isotropy, in agreement with the present analytical results.

5.3.3. *Special case of pure stratification* ($f = 0$)

In the case of pure stratification ($f = 0$), (5.9)–(5.11) become

$$\left.\begin{aligned} \overline{u_1^2}(t) &= \overline{u_2^2}(t) = KE_0 + \tfrac{1}{6}PE_0, \\ \overline{u_3^2}(t) &= \tfrac{2}{3}PE_0 - \tfrac{1}{2}PE_0\left(\frac{\pi}{Nt}\right)^{1/2}\cos\left(2Nt - \frac{\pi}{4}\right), \\ \overline{\rho^2}(t) &= N^2PE_0 + \frac{N^2}{2}PE_0\left(\frac{\pi}{Nt}\right)^{1/2}\cos\left(2Nt - \frac{\pi}{4}\right). \end{aligned}\right\} \tag{5.19}$$

These results show that, in pure stratified turbulence ($f = 0$), if the initial turbulence is axisymmetric and two-dimensional, the two-dimensionality of velocity is conserved and the initial horizontal kinetic energy can be converted neither to vertical kinetic energy nor to potential energy. On the other hand, the initial potential energy is equally partitioned between the kinetic energy $(1/2)(\overline{u_1^2} + \overline{u_2^2} + \overline{u_3^2})$ and the potential energy $(1/2N^2)\overline{\rho^2}$.

5.3.4. *Special case of* $N = f$

Similarly to initially isotropic turbulence, the method of steepest descents cannot be applied when $N = f$. However, the exact solution can be obtained as

$$\overline{u_1^2}(t) = \overline{u_2^2}(t) = \tfrac{11}{15}KE_0 + \tfrac{4}{15}PE_0 + \tfrac{4}{15}(KE_0 - PE_0)\cos Nt, \tag{5.20}$$

$$\overline{u_3^2}(t) = \tfrac{2}{15}(KE_0 + 4PE_0)(1 - \cos 2Nt), \tag{5.21}$$

$$\overline{\rho^2}(t) = \tfrac{2}{15}N^2KE_0(3 - 4\cos Nt + \cos 2Nt) + \tfrac{2}{15}N^2PE_0(7 + 4\cos Nt + 4\cos 2Nt). \tag{5.22}$$

We note again that, when $N = f$, oscillations in the variances and the covariances do not decay with time, in contrast to the case of $N \neq f$, because all the wavenumber components oscillate in phase, as discussed in the case of initially isotropic turbulence (§ 4.4.2).

It is again of interest to note that the horizontal kinetic energy contains only the slowly oscillating components and the energy exchange occurs at lower frequency N, exclusively between the horizontal kinetic energy and the potential energy, without any explicit participation of the vertical kinetic energy. On the other hand, the energy exchange at high frequency $2N$ occurs exclusively between the vertical kinetic energy and the potential energy.

6. Effects of viscosity and diffusion

When $Pr = 1$ ($\nu = \kappa$), the solutions of RDT equations which include viscosity and diffusion can be obtained simply by multiplying the spectral solutions (3.6)–

(3.9) by $\exp(-\nu k^2 t)$ and multiplying the three-dimensional spectra (3.11)–(3.14) by $\exp(-2\nu k^2 t)$. Since the value of a is not affected by viscosity and diffusion when $\nu = \kappa$, the integration by θ is unchanged. Thus the corresponding variances and covariances can be obtained simply by replacing the radial integrals

$$KE_0 = \int_0^\infty E(k)\,\mathrm{d}k \quad \text{and} \quad PE_0 = \int_0^\infty S(k)\,\mathrm{d}k \tag{6.1}$$

by

$$\int_0^\infty E(k)\exp(-2\nu k^2 t)\,\mathrm{d}k \quad \text{and} \quad \int_0^\infty S(k)\exp(-2\nu k^2 t)\,\mathrm{d}k, \tag{6.2}$$

respectively. For example when $E(k)$ and $S(k)$ are given by

$$E(k) = KE_0\left(\frac{16}{\pi}\right)^{1/2}\frac{k^2}{k_0^3}\exp(-k^2/k_0^2) \quad \text{and} \quad S(k) = PE_0\left(\frac{16}{\pi}\right)^{1/2}\frac{k^2}{k_0^3}\exp(-k^2/k_0^2), \tag{6.3}$$

as in most experiments, (6.2) becomes

$$\int_0^\infty E(k)\exp(-2\nu k^2 t)\,\mathrm{d}k = \frac{KE_0}{(1+2\nu k_0^2 t)^{3/2}}$$

$$\text{and} \quad \int_0^\infty S(k)\exp(-2\nu k^2 t)\,\mathrm{d}k = \frac{PE_0}{(1+2\nu k_0^2 t)^{3/2}}, \tag{6.4}$$

and when $E(k)$ and $S(k)$ are given by

$$E(k) = KE_0\left(\frac{2}{9\pi}\right)^{1/2}\left(\frac{2}{k_0}\right)^5 k^4\exp(-2k^2/k_0^2)$$

$$\text{and} \quad S(k) = PE_0\left(\frac{2}{9\pi}\right)^{1/2}\left(\frac{2}{k_0}\right)^5 k^4\exp(-2k^2/k_0^2), \tag{6.5}$$

(6.2) becomes

$$\int_0^\infty E(k)\exp(-2\nu k^2 t)\,\mathrm{d}k = \frac{KE_0}{(1+\nu k_0^2 t)^{5/2}}$$

$$\text{and} \quad \int_0^\infty S(k)\exp(-2\nu k^2 t)\,\mathrm{d}k = \frac{PE_0}{(1+\nu k_0^2 t)^{5/2}}. \tag{6.6}$$

7. Unstable stratification

7.1. *Variances and covariances*

So far the analysis has been for stably stratified rotating turbulence. Now we consider the unstably stratified case. When the stratification is unstable, the most unstable mode grows fastest and would become dominant. Because of the exponential growth of that mode, the turbulence energy will become large and the assumption of linearity would break down in a short time. We also note that the unstable stratification cannot sustain its initial vertical density distribution in DNS and experiments, while the RDT assumes that the unstable stratification persists. This will also make a significant difference in the results of RDT and DNS or experiments. However, it is

still of some interest to know which mechanisms work in this transition. Therefore, we give some results for unstable stratification here for later comparison with DNS and experiments in §9. The comparison will show that even for unstable stratification, the agreement between RDT and DNS is good, at least for the initial time development.

When the stratification is unstable ($N^2 < 0$), the frequency a becomes pure imaginary for

$$\theta_0 < \theta < \pi - \theta_0, \tag{7.1}$$

where

$$\theta_0 = \tan^{-1}\left(-\frac{f^2}{N^2}\right)^{1/2} \tag{7.2}$$

satisfies $0 \leqslant \theta_0 \leqslant \pi/2$.

Then for this region, we use

$$\cos at = \cosh(bt), \quad \sin at = \frac{1}{\mathrm{i}}\sinh(bt), \tag{7.3}$$

where $b = \mathrm{i}a$.

We consider in this section only initially isotropic turbulence and the variances and covariances can be obtained by using (7.3) in the unstable region. The results are, for example,

$$\overline{\rho u_3}(t) = \frac{N^2}{2}E_0^{(C)}\left(\int_0^{\theta_0} + \int_{\pi-\theta_0}^{\pi}\right)\mathrm{d}\theta\frac{\sin^3\theta}{a^3}\sin at(N^2\sin^2\theta\cos at + f^2\cos^2\theta)$$

$$+\frac{N^2}{2}E_0^{(C)}\int_{\theta_0}^{\pi-\theta_0}\mathrm{d}\theta\frac{\sin^3\theta}{b^3}\sinh bt(N^2\sin^2\theta\cosh bt + f^2\cos^2\theta). \tag{7.4}$$

We should note here that $\theta_0 \to \pi/2$ in the limit of $-N^2 \to 0$, and the integral for the unstable region (7.1) vanishes, and when $N^2 > 0$, we should use $\theta_0 = \pi/2$ in (7.4) and other similar integrals.

Other variances and covariances can be obtained similarly by dividing the integration region into a stable ($0 < \theta < \theta_0, \pi - \theta_0 < \theta < \pi$) and an unstable ($\theta_0 < \theta < \pi - \theta_0$) region. Hereafter, we assume that the integration by θ in the unstable region ($\theta_0 < \theta < \pi - \theta_0$) should use the relation (7.3) although we do not note this specifically.

7.2. *Long-time asymptotics*

When the stratification is unstable, the major contribution to the θ-integral comes from the unstable components (near $\theta = \pi/2$) and we obtain the asymptotic forms of the integral as

$$\overline{\rho u_3}(t) = -\tfrac{1}{8}|N^2|^{3/4}E_0^{(C)}\left(\frac{\pi}{t(|N^2| + f^2)}\right)^{1/2}\exp(2|N^2|^{1/2}t), \tag{7.5}$$

$$\overline{u_3^2}(t) = \tfrac{1}{8}|N^2|^{1/4}E_0^{(C)}\left(\frac{\pi}{t(|N^2| + f^2)}\right)^{1/2}\exp(2|N^2|^{1/2}t), \tag{7.6}$$

$$\overline{\rho^2}(t) = \tfrac{1}{8}|N^2|^{5/4}E_0^{(C)}\left(\frac{\pi}{t(|N^2| + f^2)}\right)^{1/2}\exp(2|N^2|^{1/2}t). \tag{7.7}$$

These show the exponential growth of the variances and the covariances. The integral for the unstable region ($\theta_0 < \theta < \pi - \theta_0$) becomes large with time and in particular the components of $\theta = \pi/2$ ($\theta_0 \leqslant \pi/2 \leqslant \pi - \theta_0$) become dominant in a long time. Therefore, the horizontal wavenumber components contribute most to the unsteadiness of the fluxes when the stratification is stable, and the same components are dominant for the unstable stratification. Note here also that since $PE_0 = (1/2N^2)\overline{\rho_0^2}$ is negative, $E_0^{(C)}$ is positive so that $\overline{\rho u_3} < 0$, $\overline{u_3^2} > 0$ and $\overline{\rho^2} > 0$. Since (7.5) includes no oscillatory components, $\overline{\rho u_3}$ does not change sign after a sufficiently long time has elapsed.

From (7.5)–(7.7) we can calculate that the normalized vertical density flux in the long-time limit as

$$\frac{\overline{\rho u_3}}{\overline{\rho^2}^{1/2}\overline{u_3^2}^{1/2}}(t \to \infty) = -1, \tag{7.8}$$

which will be compared with the DNS results in §9. We should note that this long-time limit value is independent of $E_0^{(C)}$, i.e. independent of the initial conditions.

8. Vertical vorticity

The spectral component of the vertical vorticity $\hat{\omega}_3$ is governed by the equation

$$\frac{\mathrm{d}\hat{\omega}_3}{\mathrm{d}t} = \mathrm{i}fk_3\hat{u}_3. \tag{8.1}$$

Here, the generation of vertical vorticity ω_3 or vertical absolute vorticity $\omega_3 + f$ is due to the Coriolis force ($f \neq 0$). Without system rotation, vertical vorticity simply decays through viscosity as can also be deduced directly from the linearized governing equation (2.1).

Using (3.9), the solution for $\hat{\omega}_3$ is obtained as

$$\hat{\omega}_3 = \mathrm{i}(k_1\hat{u}_{20} - k_2\hat{u}_{10}) + \mathrm{i}fk_3\left[\frac{1}{a}\hat{u}_{30}\sin at + \frac{fk_3}{a^2k^2}(k_2\hat{u}_{10} - k_1\hat{u}_{20})(1 - \cos at) + \frac{k_1^2 + k_2^2}{a^2k^2}\hat{\rho}_0(\cos at - 1)\right]. \tag{8.2}$$

Then the variance of the vertical vorticity for initially isotropic turbulence is

$$\begin{aligned}\overline{\omega_3^2}(t) &= \int \Phi_{\omega_3\omega_3}\mathrm{d}\boldsymbol{k} = \int \overline{\hat{\omega}_3\hat{\omega}_3^*}\mathrm{d}\boldsymbol{k} \\ &= \tfrac{1}{4}\overline{\boldsymbol{\omega}_0^2}\int_0^\pi \mathrm{d}\theta\frac{\sin^3\theta}{a^4}[(a^2 - f^2\cos^2\theta(1 - \cos at))^2 + a^2f^2\cos^2\theta\sin^2 at] \\ &\quad + f^2N^2\int_0^\infty \mathrm{d}k k^2S(k)\int_0^\pi \mathrm{d}\theta\frac{\sin^5\theta\cos^2\theta}{a^4}(1 - \cos at)^2,\end{aligned} \tag{8.3}$$

where

$$\overline{\boldsymbol{\omega}_0^2} = \overline{\omega_{10}^2 + \omega_{20}^2 + \omega_{30}^2} = 2\int_0^\infty k^2E(k)\,\mathrm{d}k, \tag{8.4}$$

denotes twice the initial enstrophy.

When the stratification is unstable ($N^2 < 0$), the long-time approximation is dominated by the components of $\theta \approx \pi/2$ and (8.3) becomes

$$\overline{\omega_3^2}(t) = \frac{\pi^{1/2}}{32}\frac{f^2}{|N^2|}\overline{\boldsymbol{\omega}_0^2}\frac{1}{(|N^2|^{1/2}t)^{3/2}(\frac{1}{2}+f^2/|N^2|)^{3/2}}\exp(2|N^2|^{1/2}t), \tag{8.5}$$

assuming that there is no initial potential energy ($S(k) = 0$). This result is shown here for later comparison with DNS in § 9 (figure 4).

We also consider here the effect of viscosity and diffusion for later comparison with DNS. When $Pr = 1$, the result is rather simple. For example, when the energy spectrum is given by (6.3), $\overline{\boldsymbol{\omega}_0^2}$ given by (8.4) should be simply replaced by

$$2\int_0^\infty \mathrm{d}k\, k^2 \exp(-2\nu k^2)E(k) = \overline{\boldsymbol{\omega}_0^2}\frac{1}{(1+2\nu k_0^2 t)^{5/2}}, \tag{8.6}$$

in (8.3) and (8.5).

9. Comparison with DNS and experiments

The results will now be compared with DNS and some laboratory experiments. For quantitative comparison with DNS, we should include the effects of viscosity and diffusion. We show in this section the results of RDT for $Pr = 1$. Since the previous DNS by Iida & Nagano (1999) was only for $Pr = 0.71$, a precise discussion of the Prandtl number effects are difficult. In addition, the differences due to the different Prandtl numbers are not so large as to affect the main results discussed in this section. Therefore we show the results only for $Pr = 1$.

We should note that previous DNS has used rather low Reynolds numbers. In Iida & Nagano (1999) the Reynolds number defined by $Re = k^2/(\epsilon\nu)$, where k is the kinetic energy and ϵ is the energy dissipation rate, was below 20. As noted in § 2, the low Reynolds numbers used in DNS will give better agreement with RDT than high-Reynolds numbers, since the RDT is formally not applicable to small scales of turbulence at high Re.

As regards the applicability condition of RDT, the Rossby number $Ro = \epsilon/fk$ used by Iida & Nagano (1999) is $Ro \sim 0.1$. Although the Froude number $Fr = \epsilon/Nk$ is not given explicitly in their paper, their data show $Fr \sim 1$. Thus the applicability condition given in § 2 is marginally satisfied when $f/N < 1$ and is better satisfied when $f/N > 1$ since $Ro(f/N)^{1/2} = Fr(N/f)^{1/2} \sim 0.3 < 1$ with typical value of $f/N = 10$ in their DNS.

As an initial energy spectrum $E(k)$ we use (6.3) with $k_0 = 5$, $KE_0 = 1$ and also assume $PE_0 = 0 (S(k) = 0)$, unless otherwise stated. This means that the initial turbulence is isotropic and has no density perturbations. As viscosity coefficient, we have used $\nu(=\kappa) = 0.0243$. All these conditions are the same as those in Iida & Nagano (1999) and Tsujmura *et al.* (1998) except for the value of κ.

Figure 1 shows the time development of the vertical density flux in stably stratified rotating turbulence. The RDT solutions given by (4.10) but modified by viscosity and diffusion ($Pr = 1$ ($\nu = \kappa$)) as given by (6.4) become

$$-\frac{1}{N^2}\overline{\rho u_3}(t) = -\tfrac{1}{2}E_0^{(C)}\int_0^\pi d\theta \frac{\sin^3\theta}{a^3}\sin at(N^2\sin^2\theta\cos at + f^2\cos^2\theta)\frac{1}{(1+2\nu k_0^2 t)^{3/2}}, \tag{9.1}$$

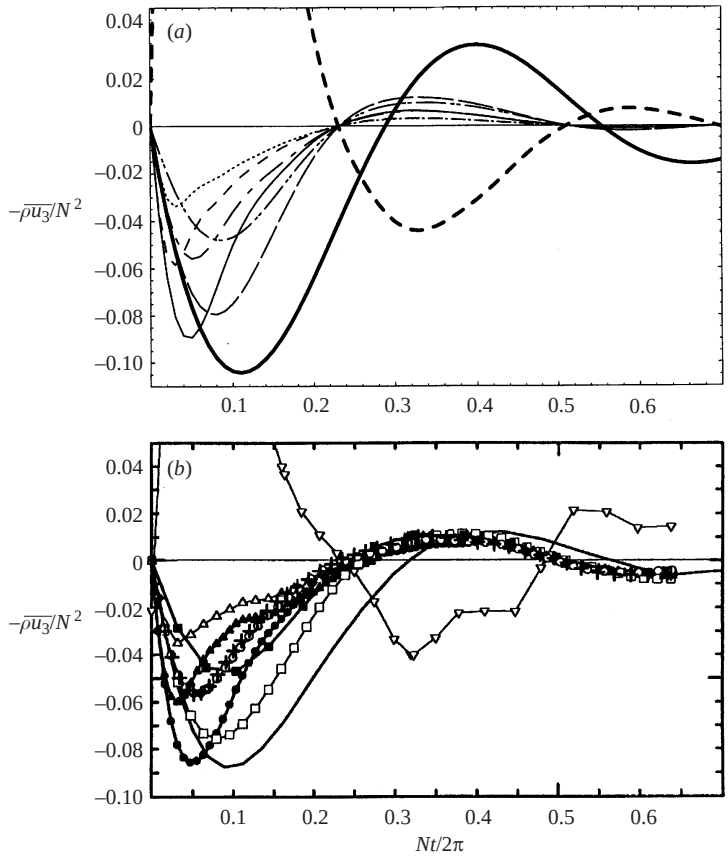

FIGURE 1. Time development of the vertical density flux $-\overline{\rho u_3}/N^2$ for initially isotropic stably stratified rotating turbulence. (*a*) RDT ($Pr = 1$): ————, $N = 2$, $f = 0$; ————, $N = 1$, $f = 10$; – – – –, $N = 1$, $f = 20$; — — —, $N = 2$, $f = 10$; —·—·—, $N = 2$, $f = 20$; ·····, $N = 2$, $f = 40$; —··—··—, $N = 4$, $f = 20$; – – – –, $PE_0 = 4KE_0$, $N = 2$, $f = 20$. (*b*) DNS by Iida & Nagano (1999) ($Pr = 0.71$): ————, $N = 2$, $f = 0$; ●, $N = 1$, $f = 10$; ▲, $N = 1$, $f = 20$; □, $N = 2$, $f = 10$; ○, $N = 2$, $f = 20$; +, $N = 2$, $f = 20$ (solution of the linearized equations); △, $N = 2$, $f = 40$; ■, $N = 4$, $f = 20$; ▽, $PE_0 \neq 0$, $N = 2$, $f = 20$.

and the long-time asymptotics given by (4.18) in combination with (6.3) become

$$-\frac{1}{N^2}\overline{\rho u_3}(t) = -\frac{1}{4N}E_0^{(c)}\left(\frac{\pi N}{t|N^2 - f^2|}\right)^{1/2}\sin\left(2Nt \pm \frac{\pi}{4}\right)\frac{1}{(1 + 2\nu k_0^2 t)^{3/2}}. \tag{9.2}$$

The overall comparison between RDT and DNS is good. There is a phase difference between the case of $N = 2$, $f = 0$ and all the other cases. When there is no rotation, $N > f$ is satisfied and the flux is proportional to $\sin(2Nt - \pi/4)$, showing phase delay. On the other hand, when rapid rotation is imposed as in all the other cases, $N < f$ is satisfied and the flux is proportional to $\sin(2Nt + \pi/4)$, showing phase advance. This is the reason why in Iida & Nagano (1999) the oscillation period appeared to be longer in the non-rotating case. The theoretical prediction of zeros by the long-time approximation are $Nt/2\pi = 0.3125, 0.5625, \ldots$ when $f < N$, and $Nt/2\pi = 0.1875, 0.4375, \ldots$ when $f > N$. The time difference in zeros is $1/8 = 0.125$. Although the method of stationary phase is a long-time approximation and is formally

applicable only at large times it gives a good approximation even for $Nt = O(1)$ as already noted in § 4.4.1.

In the very initial time development, the flux behaves as given by (4.15). When $E_0^{(C)} > 0$ or $KE_0 > 2PE_0$ is satisfied, e.g. when there is no initial potential energy, $-\overline{\rho u_3}$ initially is negative, while if large $PE_0 (> KE_0/2)$ is applied, the flux is positive. In one case ($N = 2, f = 20$), initial potential energy PE_0 is not zero. However, the values of PE_0 or the functional form of $S(k)$ are not given explicitly in Iida & Nagano (1999). Therefore, we assumed that $PE_0 = 4KE_0$ and $S(k)$ has the same form as $E(k)$ (cf. (6.3)). In that case the flux reverses its sign. As is noticable from (9.1) and (9.2), this flux reversal persists for an indefinitely long time.

As shown in (4.15), the initial time development is determined only by N as a first approximation, and the growth rate of the flux $-\overline{\rho u_3}/N^2$ (for $Nt/2\pi < 0.05$) is proportional to N^{-1} if we fix the time Nt. This is also discernible in figure 1. For the same N, the initial time development almost agrees and the growth rate is indeed proportional to N^{-1}.

At later times ($0.05 < Nt/2\pi < 0.2$) the rotation effects begin to appear, but as (9.2) suggests, the amplitude of the oscillation becomes approximately proportional to f^{-1}, provided $f \gg N$ is satisfied as in the cases shown in figure 1. This is also observed in figure 1(a, b), noting that three values are used for f (= 10, 20 and 40). The results for $f = 10$ show the largest amplitude and the results for $f = 40$ show the smallest amplitude. However, the rotation effect diminishes rapidly with time except for its effect on the amplitude and the time oscillation period ($= 2N$) is equal to twice the stratification parameter N as shown by (9.2). The amplitude difference for different values of f (and N) after a long time is smaller in DNS than RDT. One possible explanation is the effect of nonlinearity.

In figure 2 the effects of initial anisotropy (axisymmetric and purely horizontal turbulence) on stably stratified rotating turbulence are shown for the case of no initial potential energy ($PE_0 = 0$). We should note, however, that the results given here are for a special case of $N = f$ and the exact RDT solutions are (5.20) and (5.21) with the viscosity and diffusion effects ($Pr = 1$) given by (6.4), i.e.

$$\overline{u_1^2}(t) = \overline{u_2^2}(t) = [\tfrac{11}{15}KE_0 + \tfrac{4}{15}KE_0 \cos Nt]\frac{1}{(1 + 2\nu k_0^2 t)^{3/2}}, \tag{9.3}$$

and

$$\overline{u_3^2}(t) = \tfrac{2}{15}KE_0(1 - \cos 2Nt)\frac{1}{(1 + 2\nu k_0^2 t)^{3/2}}. \tag{9.4}$$

As noted in § 5.3.4, the horizontal kinetic energy $\overline{u_1^2} (= \overline{u_2^2})$ oscillates with frequency N, in contrast to the other variances and covariances. This is clearly also seen in the DNS results. However, it is important to note that this frequency difference is due to the resonant condition $N = f$ and not because of the initial anisotropy. Even when the initial turbulence is isotropic, we found the same results as described in § 4.4.2.

We should note here that the decay of the amplitude with time when $N = f$ is purely a viscosity/diffusion effect and not due to the inviscid mechanism. When $a = N = f$, all the wavenumber components in different directions (θ) oscillate in phase. Therefore, if the fluid is inviscid, the amplitude does not decay with time, in contrast to the general case of $N \neq f$. We also note that the linear results of DNS and RDT show some differences which would be due to the difference in the Prandtl number.

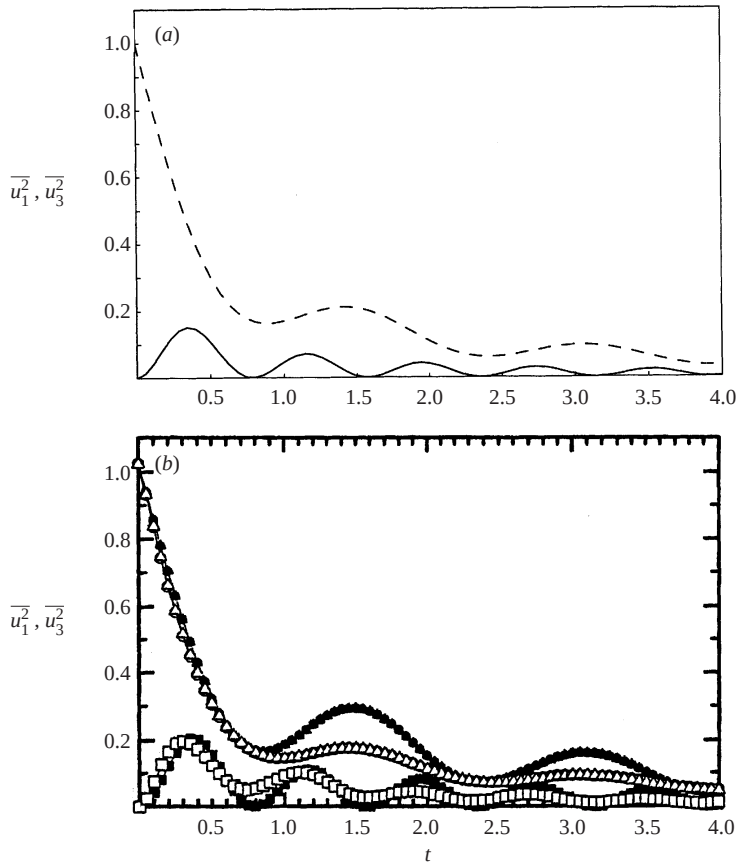

FIGURE 2. Time development of the horizontal and vertical kinetic energy for initially axisymmetric and purely horizontal stably stratified rotating turbulence with $N = f(= 4)$. (*a*) RDT ($Pr = 1$): – – – –, $\overline{u_1^2}(= \overline{u_2^2})$; ————, $\overline{u_3^2}$. (*b*) DNS by Tsujimura, Iida & Nagano (1998) ($Pr = 0.71$). nonlinear: ○, $\overline{u_1^2}$; △, $\overline{u_2^2}$; □, $\overline{u_3^2}$. linear: ●, $\overline{u_1^2}$; ▲, $\overline{u_2^2}$; ■, $\overline{u_3^2}$. 'Linear' means the solution of the linearized Navier–Stokes equations.

Figure 3 shows the time development of the normalized vertical density flux with unstable stratification with isotropic initial conditions. All the curves for $-\overline{\rho u_3}/(\overline{\rho^2}\overline{u_3^2})^{1/2}$ asymptote to 1 over a long time. RDT results (figure 3*a*) show the value calculated by (7.4) for $\overline{\rho u_3}$ and other similar expressions for $\overline{\rho^2}$ and $\overline{u_3^2}$. In the RDT results (figure 3*a*), $Pr = 1$ is used. For $Pr = 1$, the effects of viscosity and diffusion appear in the same form (e.g. $(1+2\nu k_0^2 t)^{-3/2}$ as given by (6.4)) in all the variances and covariances of the velocity and density. Therefore, the effects of viscosity and diffusion are cancelled out by the denominator and the numerator in the normalized density flux. Thus the RDT results for $Pr = 1$ actually agree with the inviscid results. For the long-time development, the asymptotics of the RDT solution give (7.5)–(7.7), which shows that $-\overline{\rho u_3}/(\overline{\rho^2}\overline{u_3^2})^{1/2} \to 1 (t \gg 1)$ as already given in (7.8). This again agrees with DNS for $PE_0 = 0$. We should recall here, as noted in § 7.2 that the value is independent of $E_0^{(C)}$, i.e. the initial condition.

In the DNS in figure 3(*b*) there are two lines for the same $|N^2|^{1/2}/f$ but for different values of $|N^2|^{1/2}$ and f. These two lines almost coincide. Examination of the RDT

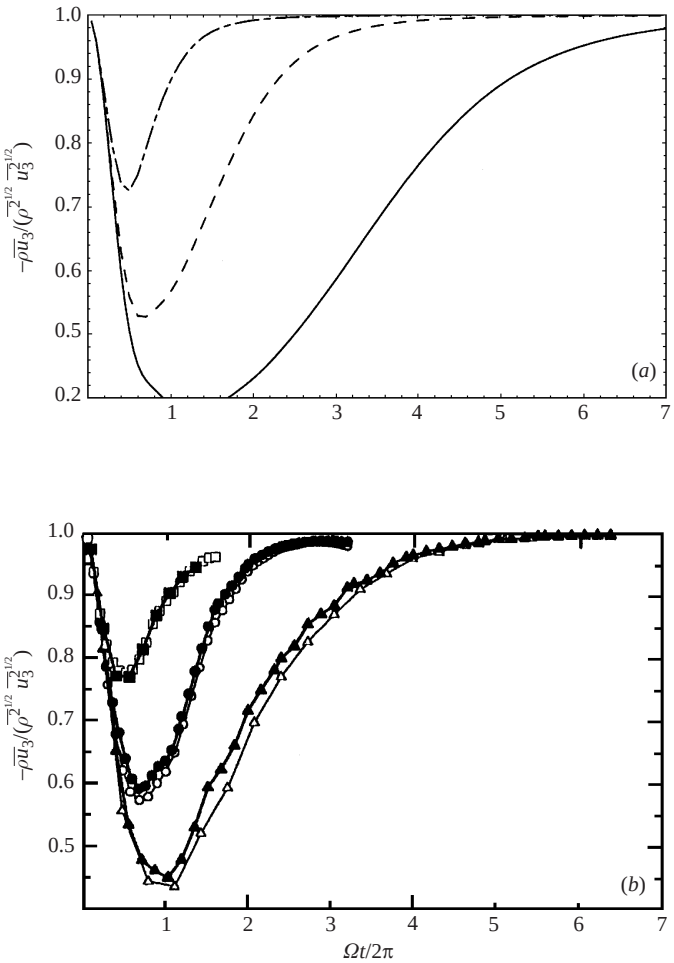

FIGURE 3. Time development of the normalized vertical density flux for initially isotropic unstably stratified rotating turbulence. (*a*) RDT ($Pr = 1$): ————, $|N^2|^{1/2}/f = 0.05$; – – – –, $|N^2|^{1/2}/f = 0.1$; —·—·—, $|N^2|^{1/2}/f = 0.2$. (*b*) DNS by Iida & Nagano (1999) ($Pr = 0.71$): △, $|N^2|^{1/2} = 2, f = 40(|N^2|^{1/2}/f = 0.05)$; ▲, $|N^2|^{1/2} = 1, f = 20(|N^2|^{1/2}/f = 0.05)$; ○, $|N^2|^{1/2} = 2, f = 20(|N^2|^{1/2}/f = 0.1)$; ●, $|N^2|^{1/2} = 1$, $f = 10(|N^2|^{1/2}/f = 0.1)$; □, $|N^2|^{1/2} = 2$, $f = 10(|N^2|^{1/2}/f = 0.2)$; ■, $|N^2|^{1/2} = 4$, $f = 20(|N^2|^{1/2}/f = 0.2)$.

solutions for the normalized vertical density flux shows that it depends on at, f/a and $|N^2|^{1/2}/f$. Since at is determined by ft and $|N^2|^{1/2}/f$ except for θ, and f/a is determined by $|N^2|^{1/2}/f$, the flux is determined only by $|N^2|^{1/2}/f$ and ft. Thus, for fixed ft, it is determined solely by $|N^2|^{1/2}/f$. The agreement of the two curves supports the importance of the linear mechanisms, showing that there are no other parameters which affect the normalized vertical density flux. Similar discussions apply to other variances and covariances.

Figure 4 shows the time development of the vertical vorticity variance for initially isotropic unstably stratified rotating turbulence. The RDT results in figure 4(*a*) show the function given by (8.3) with $S(k) = 0$ since there is no initial potential energy in DNS. Combined with the effects of viscosity and diffusion, the RDT results

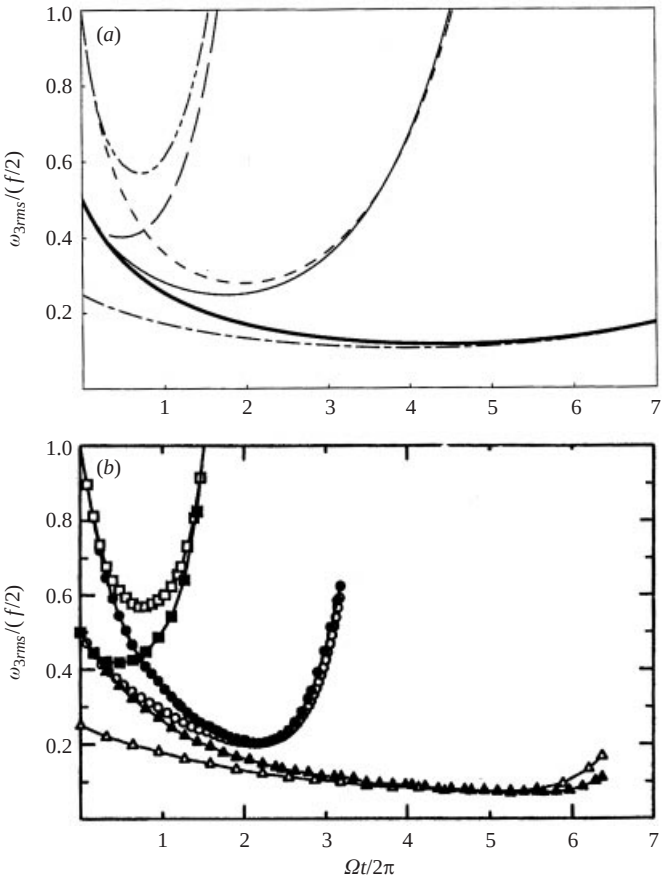

FIGURE 4. Time development of $(\overline{\omega_3^2})^{1/2}/(f/2)$ for initially isotropic unstably stratified rotating turbulence. (*a*) RDT ($Pr = 1$): —·—·—, $|N^2|^{1/2} = 2$, $f = 40(|N^2|^{1/2}/f = 0.05)$; ————, $|N^2|^{1/2} = 1$, $f = 20(|N^2|^{1/2}/f = 0.05)$; ————, $|N^2|^{1/2} = 2$, $f = 20(|N^2|^{1/2}/f = 0.1)$; – – – –, $|N^2|^{1/2} = 1$, $f = 10(|N^2|^{1/2}/f = 0.1)$; —··—··—, $|N^2|^{1/2} = 2$, $f = 10(|N^2|^{1/2}/f = 0.2)$; — — —, $|N^2|^{1/2} = 4$, $f = 20(|N^2|^{1/2}/f = 0.2)$. (*b*) DNS by Iida & Nagano (1999) ($Pr = 0.71$): △, $|N^2|^{1/2} = 2$, $f = 40(|N^2|^{1/2}/f = 0.05)$; ▲, $|N^2|^{1/2} = 1$, $f = 20(|N^2|^{1/2}/f = 0.05)$; ○, $|N^2|^{1/2} = 2$, $f = 20(|N^2|^{1/2}/f = 0.1)$; ●, $|N^2|^{1/2} = 1$, $f = 10(|N^2|^{1/2}/f = 0.1)$; □, $|N^2|^{1/2} = 2$, $f = 10(|N^2|^{1/2}/f = 0.2)$; ■, $|N^2|^{1/2} = 4$, $f = 20(|N^2|^{1/2}/f = 0.2)$.

corresponding to DNS (but with $Pr = 1$) are

$$\overline{\omega_3^2}(t) = \tfrac{1}{4}\overline{\boldsymbol{\omega}_0^2}\int_0^\pi \mathrm{d}\theta \frac{\sin^3\theta}{a^4}[(a^2 - f^2\cos^2\theta(1-\cos at))^2 + a^2 f^2\cos^2\theta\sin^2 at] \times \frac{1}{(1+2\nu k_0^2 t)^{5/2}}. \tag{9.5}$$

In the inviscid ($\nu = 0$) case, the RDT results for the vertical vorticity are again determined solely by ft and $|N^2|^{1/2}/f$. Then for fixed ft, the vertical vorticity variance depends only on $|N^2|^{1/2}/f$. Thus, in figure 4 in which $(\overline{\omega_3^2})^{1/2}/(f/2)$ is plotted instead of $(\overline{\omega_3^2})^{1/2}$, the difference due to f should appear. Indeed, both in RDT and DNS, the value of $(\overline{\omega_3^2})^{1/2}/(f/2)$ for the same $|N^2|^{1/2}/f$ but for f twice as large shows is half

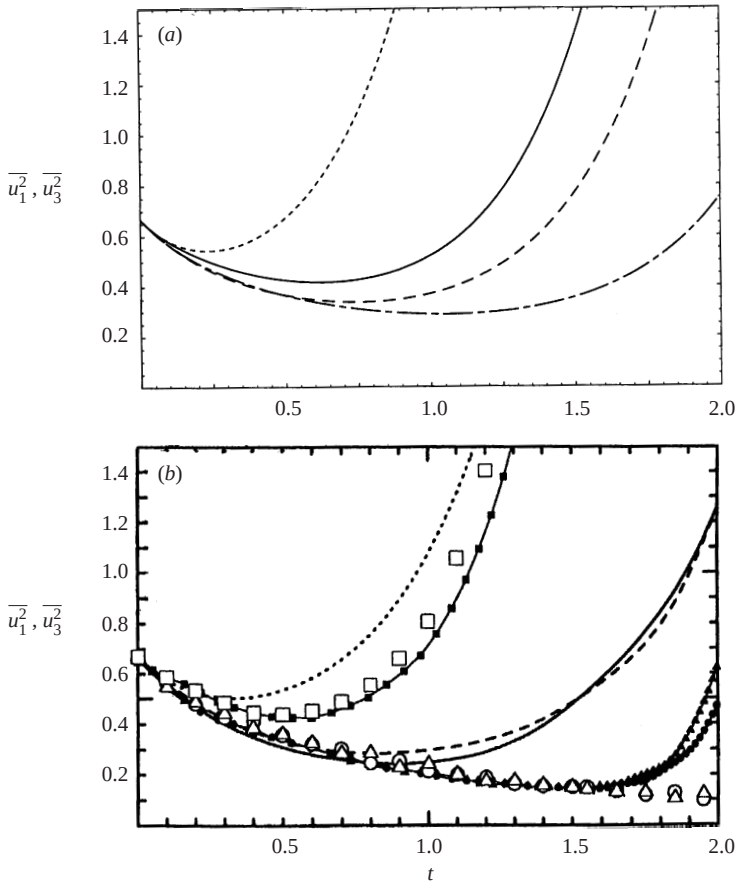

FIGURE 5. Time development of the horizontal and vertical kinetic energy for initially isotropic unstably stratified rotating and non-rotating turbulence ($|N^2|^{1/2} = 2$, $f = 20$). (*a*) RDT ($Pr = 1$): – – – –, $\overline{u_1^2}(= \overline{u_2^2})$ non-rotating; —·—·—, $\overline{u_1^2}(= \overline{u_2^2})$ rotating; ·····, $\overline{u_3^2}$ non-rotating; ————, $\overline{u_3^2}$ rotating. (*b*) DNS by Iida & Nagano (1999) ($Pr = 0.71$). Nonlinear, non-rotating: ————, $\overline{u_1^2}$; – – – –, $\overline{u_2^2}$; ·····, $\overline{u_3^2}$. Nonlinear, rotating: ●, $\overline{u_1^2}$; ▲, $\overline{u_2^2}$; ■, $\overline{u_3^2}$. Linear, rotating: ○, $\overline{u_1^2}$; △, $\overline{u_2^2}$; □, $\overline{u_3^2}$. 'Linear' means the solution of the linearized Navier–Stokes equations.

the value initially ($t = 0$). Over a long time, however, the two lines almost merge into one. This is an accidental agreement due to the effect of viscosity and diffusion. At large times, the difference (factor) due to f which can be determined from (8.5) and (8.6) is

$$\frac{1}{f(1 + 2\nu k_0^2 t)^{5/4}} \approx \frac{1}{f(2\nu k_0^2 t)^{5/4}} = f^{1/4}(2\nu k_0^2 f t)^{-5/4} (\nu k_0^2 t \gg 1). \tag{9.6}$$

For a fixed ft, the difference factor is only $f^{1/4} = 2^{1/4} = 1.189$. Although this result depends on the initial spectrum form of $E(k)$ which determines the exponent $-5/4$ in (9.6), the $E(k)$ in experiments would usually be similar to the one used here. Therefore, agreement is expected also in the experiments. We note also that the initial decay of vertical vorticity is due to the viscosity and diffusion. Indeed, the inviscid RDT shows a monotonic increase although the results are not presented here.

Figure 5 shows the time development of the kinetic energies for initially isotropic unstably stratified rotating turbulence with no initial potential energy ($PE_0 = 0$). The

RDT results are plotted using equations (4.11) and (4.12) combined with the effect of viscosity and diffusion given by (6.4), i.e.

$$\overline{u_1^2}(t) = \overline{u_2^2}(t) = \left[\tfrac{2}{3}KE_0 + \frac{N^2}{8}KE_0\int_0^\pi \mathrm{d}\theta \frac{\sin^3\theta\cos^2\theta}{a^4}(4f^2\cos^2\theta(\cos at - 1) + (f^2 - N^2)\sin^2\theta(1-\cos 2at))\right]\frac{1}{(1+2\nu k_0^2 t)^{3/2}}, \tag{9.7}$$

$$\overline{u_3^2}(t) = \left[\tfrac{2}{3}KE_0 - \frac{N^2}{2}KE_0\int_0^\pi \mathrm{d}\theta \frac{\sin^5\theta}{a^2}\sin^2 at\right]\frac{1}{(1+2\nu k_0^2 t)^{3/2}}. \tag{9.8}$$

Initial decay is again due to the viscosity of the fluid. Inviscid RDT gives a monotonic increase of both the horizontal and vertical kinetic energies. However, the viscosity and diffusion contribute to the short-time approximation (4.15) by the factor

$$\frac{1}{(1+2\nu k_0^2 t)^{3/2}} \approx 1 - 3\nu k_0^2 t = 1 - O(t)\ (\nu k_0^2 t \ll 1), \tag{9.9}$$

showing that the viscosity effects appear in the leading-order correction to the kinetic energies, compared to the effect of unstable stratification whose order is $(Nt)^2$. Then, in the initial time development, the effect of viscous damping appears first and then the growth due to unstable stratification appears at later times. We should note that the behaviour depends on the initial energy spectrum form and the viscosity coefficient, but whatever the initial spectrum forms are, the viscous decay appears at $O(t)$, faster than unstable stratification effects. The initial decay is stronger in the horizontal kinetic energy $\overline{u_1^2}$ than in the vertical kinetic energy $\overline{u_3^2}$. As is apparent in (4.15), the coefficient of $(Nt)^2$ which represents the effect of unstable stratification is $1/15$ for $\overline{u_1^2}$, while it is $8/15$ for $\overline{u_3^2}$. Thus the growth is more significant in $\overline{u_3^2}$. In experiments for non-rotating unstably stratified fluids Nagata & Komori (2000) (see their figure 2*a*) found similar behaviour.

10. Conclusions

In this study we have solved the RDT equations for both stably and unstably stratified rotating turbulence when the initial turbulence is either isotropic or axisymmetric. The importance of the initial condition has been confirmed as in stratified non-rotating turbulence. For example, the ratio of the initial potential energy to the kinetic energy determines the direction of the vertical density flux, and in viscous flow, the initial spectrum forms determine the decay rates of the energies and the fluxes. We found good agreement with the previous DNS by Iida & Nagano (1999) in many aspects and also with Bartello (1995) for the prediction of the energy partition.

The rotation modifies the energy partition among the kinetic energy components and the potential energy, and the ratio of the Coriolis parameter f to the Brunt–Väisälä frequency N, i.e. f/N, determines the final steady values, in combination with the initial kinetic energy KE_0 and the initial potential energy PE_0. The final steady value of KE/PE for the same parameters as used in DNS by Bartello (1995) gave good agreement, confirming that the linear processes are dominant in decaying stratified rotating turbulence.

However, the effects of rotation on the 'unsteady' aspects of the stratified turbulence are not very large. The long-time asymptotics show that the energy components and the fluxes oscillate at the same frequency $2N$ as the non-rotating stratified

turbulence. This is because the Coriolis parameter f is always coupled with $\cos\theta$ or the vertical wavemumber k_3 in the form of $f\cos\theta$ or fk_3, which vanishes for the angle $\theta = \pi/2$ dominantly contributing to the variances and the covariances. The wavenumber direction that contributes most, i.e. the horizontal direction ($k_3 = 0$) or the barotropic mode, is the same as for non-rotating stratified turbulence. Therefore, the stratification effects dominate in the unsteady aspects of turbulence even with the system rotation.

Short-time approximations also show that very initial time development of the energies and the fluxes are determined dominantly by stratification. Therefore, rotation effects are significant for a relatively short time, as observed in the time development of the vertical heat flux in DNS. These characteristics lead to the result that the normalized vertical density flux for the short-time limit ($t \to 0$) is the same as for non-rotating stratified fluids.

Long-time-limit steady values of the energies and the fluxes of course depend on the ratio of N and f. However, if $f \ll N$ holds, as in the atmosphere and the ocean, those asymptotic values agree approximately with the pure stratification results ($N \neq 0, f = 0$) given by Hanazaki & Hunt (1996). For example, energy ratio *ER*, the ratio of the potential energy to the vertical kinetic energy, approaches $3/2$ over a long time, irrespective of the initial conditions. One interesting effect of the ratio f/N is that it determines the 'phase' of oscillation in the energy and the fluxes. If $f/N > 1$, there is a phase advance ($+\pi/4$), while if $f/N < 1$, there is a phase delay ($-\pi/4$).

In the special case of $N = f$, the time oscillations of the energies and the fluxes do not show inviscid decay like $\propto t^{-1/2}$ as observed in the general case of $N \neq f$, which includes the case of pure stratification ($f = 0$) (Hanazaki & Hunt 1996). Thus the energy components never reach constant values in inviscid fluid in this case. This is because all the wavenumber components oscillate in phase, irrespective of their directions so that the contributing components are not restricted to the horizontal wavenumbers. We note that, in this case, the exchange between the horizontal kinetic energy and the potential energy occurs at low frequency N, and the horizontal energies $\overline{u_1^2}$ and $\overline{u_2^2}$ oscillate at that frequency. On the other hand, the energy exchange at the normal high frequency $2N$ occurs exclusively between the vertical kinetic energy and the potential energy.

In the case of pure rotation ($f \neq 0, N = 0$), the analytical solutions from RDT showed that any turbulence that is initially axisymmetric around the vertical axis returns to isotropy by linear mechanisms. This is in agreement with the DNS and the numerical solutions of RDT equations with viscosity (Cambon & Jacquin 1989).

The normalized vertical density flux $\overline{\rho u_3}/(\overline{\rho^2}\,\overline{u_3^2})^{1/2}$ depends only on the parameter $|N^2|^{1/2}/f$ and time ft, and the results for different values of $|N^2|^{1/2}$ and f give the same value in both the RDT and the DNS, supporting the dominance of the linear processes.

The long-time r.m.s. value of the vertical vorticity divided by $f/2$, i.e. $\overline{\omega_3^2}/(f/2)$, also depends almost only on the parameter $|N^2|^{1/2}/f$ and time ft, independent of the specific values of $|N^2|^{1/2}$ and f. This again has been observed in RDT and DNS, but it could be explained in RDT solutions that it has been an accidental result due to the viscosity/diffusion effects and with the specific initial energy spectral form.

It is of interest to note that the time development of even the small-scale characteristics of turbulence as represented by vertical vorticity could be explaind well by RDT, although further studies on the energy spectra would be necessary to pursue this point.

The RDT for unstably stratified results shows that the initial decay in the time development of the kinetic energy components is due to viscosity effects which become dominant initially and the growth due to unstable stratification appears at later times. This also agrees with the DNS and the experiments. This shows that the linear processes described by RDT are dominant at least for a relatively short time before the exponential growth of turbulence due to instability and the subsequent nonlinear saturation of the growth become dominant for $|N^2|^{1/2}t > O(1)$.

We should note that the DNS data mainly used for comparison with RDT in this study have been for low Reynolds numbers, which will make the comparison better. As shown in § 2, the RDT is not applicable to the small scales at high Re. Thus, in interpreting the results given in this study in the context of real atmosphere or oceans, we should take care with the applicability conditions, since Re is usually very high there.

We finally note that in DNS and in the theoretical RDT, the initial conditions are usually restricted to idealized ones, such as isotropic turbulence. In real geophysical contexts, the initial conditions are usually more complicated depending on how the turbulence is generated. Therefore, care should be taken that results obtained under idealized conditions are applicable only to those specific initial conditions.

REFERENCES

Babin, A., Mahalov, A., Nicolaenko, B. & Zhou, Y. 1997 On the asymptotic regimes and the strongly stratified limit of rotating Boussinesq equations. *Theoret. Comput. Fluid Dyn.* **9**, 223–251.

Bardina, J., Ferziger, J. H. & Rogallo, R. S. 1985 Effect of rotation on isotropic turbulence: computation and modelling. *J. Fluid Mech.* **154**, 321–336.

Bartello, P. 1995 Geostrophic adjustment and inverse cascades in rotating stratified turbulence. *J. Atmos. Sci.* **52**, 4410–4428.

Batchelor, G. K. & Proudman, I. 1954 The effect of rapid distortion on a fluid in turbulent motion. *Q. J. Mech. Appl. Maths* **7**, 83–103.

Cambon, C. & Benoit, J. P., Shao, L. & Jacquin, L. 1994 Stability analysis and LES of rotating turbulence with organized eddies. *J. Fluid Mech.* **278**, 175–200.

Cambon, C. & Jacquin, L. 1989 Spectral approach to non-isotropic turbulence subjected to rotation. *J. Fluid Mech.* **202**, 295–317.

Cambon, C., Mansour, N. N. & Godeferd, F. S. 1997 Energy transfer in rotating turbulence. *J. Fluid Mech.* **337**, 303–332.

Cho, J. Y. N., Newell, R. E. & Barrick, J. D. 1999 Horizontal wavenumber spectra of winds, temperature, and trace gases during the Pacific Exploratory Missions: 2. Gravity waves, quasi-two-dimensional turbulence, and vortical modes. *J. Geophys. Res.* **104**, 16297–16308.

Derbyshire, S. H. & Hunt, J. C. R. 1993 Structure of turbulence in stably stratified atmospheric boundary layers; Comparison of large eddy simulations and theoretical results. In *Waves and Turbulence in Stably Stratified Flows* (ed. S. D. Mobbs & J. C. King), pp. 23–59. Clarendon Press.

Embid, P. F. & Majda, A. J. 1996 Averaging over fast gravity waves for geophysical flows with arbitrary potential vorticity. *Commun. Partial Diffl Equat.* **21**, 619–658.

Embid, P. F. & Majda, A. J. 1998 Low Froude number limiting dynamics for stably stratified flow with small or finite Rossby numbers. *Geophys. Astrophys. Fluid Dyn.* **87**, 1–50.

Galmiche, M. & Hunt, J. C. R. 2002 The formation of shear and density layers in stratified turbulent flows: linear processes. *J. Fluid Mech.* **455**, 243–262.

Gerz, T. & Yamazaki, H. 1993 Direct numerical simulation of buoyancy-driven turbulence in stably stratified fluid. *J. Fluid Mech.* **249**, 415–440.

Greenspan, H. P. 1968 *The Theory of Rotating Fluids.* Cambridge University Press.

Hanazaki, H. 2000 On the transport mechanisms in stably stratified rotating turbulence. In *Turbulence, Heat and Mass Transfer 3* (ed. Y. Nagano, K. Hanjalic & T. Tsuji), pp. 639–644. Aichi Shuppan.

Hanazaki, H. & Hunt, J. C. R. 1996 Linear processes in unsteady stably stratified turbulence. *J. Fluid Mech.* **318**, 303–337.

Hanazaki, H. & Hunt, J. C. R. 2001 Linear processes in unsteady stratified sheared turbulence. *IUTAM Symp. on Geometry and Statistics of Turbulence* (ed. T. Kambe, T. Nakano & T. Miyauchi), pp. 291–296. Kluwer.

Herring, J. R. 1974 Approach of axisymmetric turbulence to isotropy. *Phys. Fluids* **17**, 859–872.

Hinch, E. J. 1991 *Perturbation Methods.* Cambridge University Press.

Hunt, J. C. R., Kaimal, J. C. & Gaynor, J. E. 1985 Some observations of turbulence structure in stable layers. *Q. J. R. Met. Soc.* **111**, 793–815.

Hunt, J. C. R., Stretch, D. D. & Britter, R. E. 1988 Length scales in stably stratified turbulent flows and their use in turbulence models. In *Stably Stratified Flow and Dense Gas Dispersion* (ed. J. S. Puttock), pp. 285–321. Clarendon Press.

Iida, O. & Nagano, Y. 1999 Coherent structure and heat transfer in geostrophic flow under density stratification. *Phys. Fluids* **11**, 368–377.

Itsweire, E. C., Helland, K. N. & Van Atta, C. W. 1986 The evolution of grid-generated turbulence in a stably stratified fluid. *J. Fluid Mech.* **162**, 299–338.

Kaneda, Y. 2000 Single-particle diffusion in strongly stratified and/or rapidly rotating turbulence. *J. Phys. Soc. Japan* **69**, 3847–3852.

Kaneda, Y. & Ishida, T. 2000 Suppression of vertical diffusion in strongly stratified turbulence. *J. Fluid Mech.* **402**, 311–327.

Kimura, Y. & Herring, J. R. 1996 Diffusion in stably stratified turbulence. *J. Fluid Mech.* **328**, 253–269.

Komori, S. & Nagata, K. 1996 Effects of molecular diffusivities on counter-gradient scalar and momentum transfer in strongly stable stratification. *J. Fluid Mech.* **326**, 205–237.

Komori, S., Ueda, H., Ogino, F. & Mizushina, T. 1983 Turbulence structure in stably stratified open-channel flow. *J. Fluid Mech.* **130**, 13–26.

Lienhard, J. H. & Van Atta, C. W. 1990 The decay of turbulence in thermally stratified flow. *J. Fluid Mech.* **210**, 57–112.

Lilly, D. K. 1983 Stratified turbulence and the mesoscale variability of the atmosphere. *J. Atmos. Sci.* **40**, 749–761.

McWilliams, J. C. 1985 A uniformly valid model spanning the regimes of geostrophic and isotropic, stratified turbulence: Balanced turbulence. *J. Atmos. Sci.* **42**, 1773–1774.

Majda, A. J. & Grote, M. J. 1997 Model dynamics and vertical collapse in decaying strongly stratified flows. *Phys. Fluids* **9**, 2932–2940.

Mansour, N. N., Shih, T.-H. & Reynolds, W. C. 1991 The effects of rotation on initially anisotropic homogeneous flows. *Phys. Fluids* A **3**, 2421–2425.

Métais, O., Bartello, P., Garnier, E., Riley, J. J. & Lesieur, M. 1996 Inverse cascade in stably stratified rotating turbulence. *Dyn. Atmos. Oceans* **23**, 193–203.

Métais, O. & Herring, J. 1989 Numerical simulations of freely evolving turbulence in stably stratified fluids. *J. Fluid Mech.* **202**, 117–148.

Nagata, K. & Komori, S. 2000 The effects of unstable stratification and mean shear on the chemical reaction in grid turbulence. *J. Fluid Mech.* **408**, 39–52.

Nieuwstadt, F. T. M. 1984 The turbulent structure of the stable, nocturnal boundary layer. *J. Atmos. Sci.* **41**, 2202–2216.

Pearson, H. J. & Linden, P. F. 1983 The final stage of decay of turbulence in stably stratified fluid. *J. Fluid Mech.* **134**, 195–203.

Riley, J. J. & Lelong, M. P. 2000 Fluid motions in the presence of strong stable stratification. *Annu. Rev. Fluid Mech.* **32**, 613–657.

Riley, J. J., Metcalfe, R. W. & Weissman, M. A. 1981 Direct numerical simulations of homogeneous turbulence in density stratified fluids. *Nonlinear Properties of Internal Waves. AIP Conference Proc.* vol. 76, pp. 79–112. American Institute of Physics.

Salhi, A. & Cambon, C. 1997 An analysis of rotating shear flow using linear theory and DNS and LES results. *J. Fluid Mech.* **347**, 171–195.

Schumann, U. & Patterson, G. S. 1978 Numerical study of the return of axisymmetric turbulence to isotropy. *J. Fluid Mech.* **88**, 711–735.

Shih, T.-H., Reynolds, W. C. & Mansour, N. N. 1990 A spectrum model for weakly anisotropic turbulence. *Phys. Fluids* A **2**, 1500–1502.

Staquet, C. & Godeferd, F. S. 1998 Statistical modelling and direct numerical simulations of decaying stably stratified turbulence. Part 1. Flow energetics. *J. Fluid Mech.* **360**, 295–340.

Townsend, A. A. 1976 *The Structure of Turbulent Shear Flow*. Cambridge University Press.

Tsujimura, S. Iida, O. & Nagano, Y. 1998 Effects of rotation on unstably stratified turbulence. *Proc. Intl Conf. on Turbulent Heat Transfer 2, Manchester, UK*, vol. 1, pp. 5-58–5-71.

Van Zandt, T. E. 1982 A universal spectrum of buoyancy waves in the atmosphere. *Geophys. Res. Lett.* **9**, 575–578.

Whitham, G. B. 1974 *Linear and Nonlinear Waves*. John Wiley & Sons.

Yoon, K. & Warhaft, Z. 1990 The evolution of grid generated turbulence under conditions of stable thermal stratification. *J. Fluid Mech.* **215**, 601–638.